INVESTIGATIONS ON GAMMA RAY

INTERACTIONS

USING ^{137}CS GAMMA RAYS

Thesis submitted to the University of Calicut

In partial fulfillment of the requirements

for the Degree of

DOCTOR OF PHILOSOPHY

IN PHYSICS

By

KARUNAKARAN NAIR K.

DEPARTMENT OF PHYSICS
UNIVERSITY OF CALICUT

2003

TO

MY PARENTS

AND

TEACHERS

Dr. K. M. Varier   Department of Physics
Professor   University of Calicut

CERTIFICATE

This is to certify that this thesis entitled `Investigations on gamma ray interactions using ^{137}Cs gamma rays' is a bonafide record of research work carried out by Karunakaran Nair.K under my supervision in the Department of Physics, University of Calicut, for the award of the Ph. D degree of University of Calicut and that no part of this thesis has been presented elsewhere for the award of any degree, diploma or other similar title.

Calicut University

7th May 2003   (Dr. K. M. Varier)

3

DECLARATION

I hereby declare that this thesis entitled ` Investigations on gamma ray interactions using ^{137}Cs gamma rays' is a bonafide record of research work done by me and that no part of this thesis has been presented before for the award of any degree or diploma.

Calicut University
7th May 2003

(Karunakaran Nair K.)

4

ACKNOWLEDGEMENTS

Karunakaran Nair K.

5

LIST OF FIGURES

LIST OF TABLES

PAPERS PUBLISHED IN JOURNALS

1. "Possible effect of source backing on back scatter peak in gamma spectra", Varier K.M. and Karunakaran Nair K., Radiat. Phys. Chem., 51 (1998) 461

PAPERS PRESENTED AT CONFERENCES

1. "Possible effect of source backing on back scatter peak in gamma spectra",Varier K.M. and Karunakaran Nair K, 7 th International symposium on Radiation Physics – ISRP – 7, Jaipur , June 1997, p 461

2. "Effect of absorber Position on Gamma ray spectra" ,Karunakaran nair.K, Unnikrishnan M.P, Varier K.M ,13 th National Symposium on Radiation Physics , Mangalore, December 1999, p. 547

3. "Gamma ray Attenuation measurement in leaf and Wood Samples" Ramachandran N. , Karunakaran Nair.K , Varier K.M, 14 th National Symposium on Radiation Physics, Amritsar, November 2001, p 142

4. "Effective atomic number by gamma ray absorption studies", Karunakaran Nair.K , Abdul Gafoor A.K. Jeeja V.S., Ramachandran N. and Varier K.M, 14 th National Symposium on Radiation Physics, Amritsar, November 2001, p 137

5. "Gamma attenuation studies in liquid nitrogen", Karunakaran Nair.K , Ramachandran N. and Varier K.M, 14 th National Symposium on Radiation Physics, Amritsar, November 2001, p 145

CONTENTS

INTRODUCTION

CHAPTER I

INTRODUCTION

Gamma radiations are electromagnetic waves having very high frequency. Hence they possesses high energy, ranging from a few keV to several MeVs. They interact with matter either through a scattering process or through an absorption process. When gamma radiation interacts with matter through scattering, a photon is deflected out of the beam, transferring a part of its energy and momentum to this interacting system. In the absorption process there is a direct conversion of the photon energy as a whole or part in to kinetic energy of one or more of the constituents.

Absorption of gamma rays by matter can take place by one of the following processes. In the photoelectric process, the incident gamma ray photon transfers all its energy to a bound electron in an atom. The bound electron uses part of this energy to overcome the binding in the atom and the remaining energy is carried as its kinetic energy. The photoelectric absorption probability increases with the tightness of electron binding and hence chiefly involves the K-shell. K-shell photoelectric effect is possible only for photons possessing energies greater than K- electron binding energy. The photoelectric absorption cross section in the K- shell of an atom with atomic number Z is proportional to Z^5. The photoelectric process predominates at low energies (up to 500 keV).

If the incident gamma ray photon is completely absorbed by the pair production process, simultaneous creation of an electron - positron pair occurs. This process has a threshold at 1.02 MeV and as the energy increases this becomes a dominant mode of interaction. The total kinetic energy of the resultant particles is equal to the incident photon energy minus the total mass energy of the two particle created. The nuclear pair production cross section is proportional to Z^2.

Nuclear photo effect, also known as photonuclear absorption, is energetically possible whenever the incident photon energy exceeds the separation energy of a proton or neutron. This process starts only if the incident photon energy exceeds about 10 MeV.

If the incident photon energy is above about 150 MeV, photo-meson production starts. However, the cross sections are very small.

When we consider the scattering of gamma ray photon it can be of two types: elastic and inelastic. In elastic scattering the scattered photon possesses nearly the same energy as the incident photon except for a negligibly small recoil energy taken by the scattering atom. There are four types of elastic scattering processes.

Rayleigh scattering is from bound atomic electrons. It is important in the region around and below 1MeV. Also, this effect is largest at small scattering angles.

Nuclear Thomson scattering takes place at energies low compared to nuclear mass and it is independent of energy and is propotional to Z^4. Nuclear Thomson Scattering is scattering from the nucleus as a whole and is a coherent scattering process.

In nuclear resonance scattering, excitation of a nuclear level by the incident photon takes place with the subsequent re-emission of the excitation energy as a gamma ray photon. It is significant in the regions of narrow resonance maxima at low energies and board maxima in the range of 10 to 30 MeV. The latter case is called Giant Dipole Resonance(GDR). The probability for this process varies as Z^2. The interaction of gamma rays with Coulomb field of the nucleus is known as Delbruck scattering. According to optical theorem, the imaginary Delbruck amplitude vanishes below the pair production threshold of 1.02 MeV.

Gamma rays also experience inelastic scattering from bound electrons in the atom. The scattered gamma ray possesses less energy compared to the incident photon. At energies less than 1 MeV, this process dominates. The cross section varies as Z. At energies greater than about 10 MeV incoherent scattering from individual nucleus takes place.

It is possible for an inner-shell electron to be virtually excited to positive energy continuum state by an incident photon at energies close to, but less than, inner shell thresholds. The resulting vacancy is filled by an electron from higher

shells with the emission of a photon. This process is known as resonant Raman scattering. We can describe Rayleigh scattering using form factor approximation [1]. In this form factor approximation (FFA), the differential cross section is expressed in terms of the atomic form factor. Close to the absorption edge energies, there is a departure from the FFA. This departure from FFA, which depends on photon energy, is called anomalous scattering contribution or dispersion corrections. This anomalous scattering of X– rays is important in the interpretation of diffraction photographs.

When a beam of photons is incident on a material, the gamma rays undergo interaction with the atoms of the material. The gamma ray photons are removed or transmitted individually from the incident beam by the interaction events which may be due to any of the process listed above. As the photons traverses through the material medium they are continuously removed from the beam. This reduction in the intensity of the gamma ray can be expressed as [2]

$$I = I_0 \exp(-\mu t)$$
.........(1.1)

where I_o is the initial intensity, I the intensity after traversing a thickness t through the material, μ is the total linear attenuation coefficient. μ can be expressed in barns / atom as follows.

$$\sigma = (\mu / \rho)(A/N_o) 10^{24}$$
.......(1.2)

where ρ is the density, A the atomic weight and N_o the Avogadro number. It is better to use the mass attenuation coefficient μ/ρ instead of ρ since the interaction cross section is then unaffected by the density of the interacting medium. The total attenuation cross section of a compound system (σ_{comp}) in terms of the cross section σ_i of its various atomic constituents is

$$\sigma_{comp} = \sum_i n_i \sigma_i \qquad \ldots\ldots\ldots(1.3)$$

Since the total interactions are unaffected by chemical combination n_i is the number of atoms of ith element present in the compound . This mixture rule [2] ignores the changes in the wave function resulting from the changes in chemical, molecular and crystalline environment of the atom. When the incident energy is very high compared to absorption edge energies, the mixture rule holds to fairly good accuracy but at low absorption edge energies the error from these approximation is large. Now μ can be expressed as

$$\mu = \mu_a + \mu_s \qquad \ldots\ldots\ldots(1.4)$$

μ_a and μ_s being respectively contribution from absorption and scattering. If the energy is below 1.02 MeV, absorption is due to photoelectric effect and $\mu_a = \mu_{ph}$. Hence if μ_s is known, μ_{ph} can be calculated by measuring μ.

By doing an absorption measurement experiment, the total absorption coefficient can be determined. For this we should know how many photons traversed through certain thickness without undergoing any interaction. In a transmission experiment a photon once scattered in the absorber even at very small angle should not be detected. The narrow beam geometry [3] enables this and is usually used to measure gamma ray attenuation coefficients. This narrow beam geometry reduces the sold angle subtend by the detector at the centre of the absorber by use of suitable collimator and shielding. This technique prevents coherently or incoherently scattered photons from reaching the detector. Hence only those photons which travel through the absorber with out any interaction are detected.

In many areas of research photon attenuation and scattering data are required. They are of importance in areas of studies such as radiation transport and shielding. information regarding scattering amplitude is necessary in sold state structure studies such as X-ray diffraction in crystalline solids and "EXAFS" analysis in amorphous materials etc.

Information of accurate Rayleigh scattering amplitude is important In the investigation of Delbruck scattering , X-ray diagnostics [4] and narrow beam attenuation studies. Attenuation studies on gamma rays in broad beam condition is important in radio biology and radio therapy [5].

Accurate measurements of X-ray attenuation coefficients is necessary because of the rapid advances made in analytical methods using X-rays. The PIXE (Proton induced X – ray emission) technique of trace element analysis is an example of trace methods [6]. Careful measurements [7] of the attenuation coefficients give important data on composition of materials or tissues. Based on attenuation coefficient studies, elemental analysis [8] also can be carried out.

In the present work, the aim is to study certain aspects of gamma ray interactions with matter. More stress has been given for determination of attenuation coefficients of different materials. The gamma ray energy of 661.6 keV has been chosen for these investigations. It was obtained using a ^{137}Cs radioactive source.

In the following, chapter II deals with descriptions of the various processes by which gamma rays interact with matter. It also describes about gamma ray attenuation. In chapter III, a detailed review of some of the important previous investigations on gamma ray attenuation is presented. Chapter IV deals with the details of some preliminary measurements on gamma ray attenuation. Specifically, a comparison is given between narrow beam and broad beam geometry measurements. In chapter V are presented the details of the experiments and the results of measurements aimed at studying the effect of the absorber position on gamma ray attenuation measurements. The concept of the effective atomic number with respect to measured gamma attenuation coefficients is described in chapter VI. The investigations carried out in the present work in this direction are described in detail in this chapter. The next two

chapters describe some measurements wherein the effective gamma transmission through the absorber changes with time. In chapter VII, the details of the measurements using liquid nitrogen are given. In the same chapter, some studies involving flowing water are also presented. In the next chapter, the idea of using rotating absorbers to simulate mixed absorbers is presented. Finally, in the last chapter, the effect of source backing on the back scatter peak in the pulse height spectra of mono energetic gamma rays is discussed. The details of the experiments carried out in this field and the results obtained there from are discussed in this last chapter.

REFERENCES

1. Debye P., Zeit. Phys. 31, 419 (1930)

2. Evans R.D., "The Atomic Nucleus" (McGraw Hill, 1955) p. 713

3. Hubbel J.H., NSRDS Report – NBS 529 (1969)

4. Henke. B.L., "low energy X-ray Diagnostics" (1981), ed. D.T.Attwood and B.L. Henke, AIP Conference Proc. No 75

5. Van Dyk J., Med. Phys. 13 (1986) 105

6. Varier K.M., Mehta G.K. and Sen. S, Phys. News 11 (1980) 1

7. Cesareo R. and Gianini. M, Nucl. Inst. And Meth. 169 (1980) 551

8. Kouris. K. and Spyrou. N., Nucl. Inst. And Meth., 153 (1978) 477

GAMMA RAY INTERACTIONS

Chapter II

GAMMA RAY INTERACTIONS

2.1 Introduction.

In the present work we are using gamma rays of the order of 1 MeV. In this energy range, gamma ray interactions are primarily due to absorption from photoelectric effect and pair production and scattering by atomic electrons. At energies less than 500 keV, photoelectric effect gives the chief contribution in the case of heavy elements like lead. As energy increases, Compton scattering becomes increasingly more prominent as compared to the photoelectric effect and this is the main process contributing to the absorption coefficient. This process is important in the region above 50 keV and less than 15 MeV for a light element like aluminium and in the range 0.5 MeV to 5 MeV for a heavy element such as lead. At high energies, pair production is the dominant process. At low gamma energies and in high Z materials, Rayleigh scattering makes important contribution to the attenuation of gamma rays.

In the following sections, some details about these various processes are presented.

2.2 Photoelectric effect

Fig 2.1 gives the diagrammatic representation of this process. When photoelectric effect takes place, the energy of the emitted electron is given by

$$E_e \quad = \quad E_\gamma - E_b \qquad \ldots\ldots\ldots\ldots(2.1)$$

E_γ is the energy of photon and E_b is the binding energy of the electron ejected. If the photon energy is less than K – shell binding energy, ejection of K – shell electron does not take place but L, M shell electrons can interact. Hence the probability for photoelectric absorption falls sharply as the photon energy decreases through the K edge and similar discontinuities occur at binding energies of L,M etc shells.

The photoelectric cross section depends on the gamma energies and Z of the material used. The cross section increases as Z increases and is proportional to Z^n. Depending on gamma energy, the exponent n varies from 4 to 5. The photoelectric effect cross section decreases as the energy E rises. At low energies it is proportional to $1/E^3$ and at E> 0.5 MeV the variation is 1/E. Hence for high Z elements and at low gamma energies the photoelectric effect predominates.

If the absorber is thick, the auger electrons and fluorescent X – rays which may be produced are usually reabsorbed. The photoelectrons are emitted usually in a direction at right angles to the direction of the incident photon. When the photon energy increases the angular distribution tends to maximize more in the forward direction.

Photoelectron

e

Incident
Photon

Z
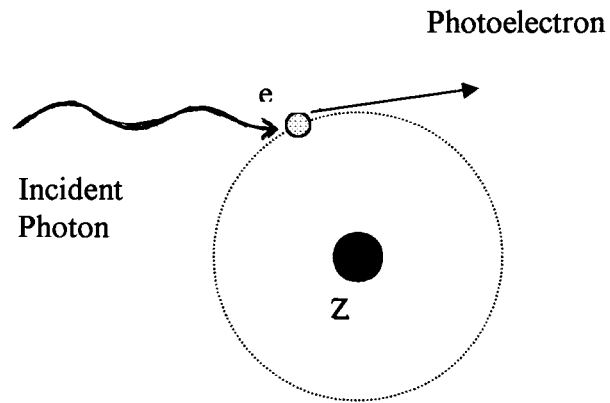
Fig 2.1 Schematic diagram of the Photo electric effect

2.3 Pair production

In this process, production of an electron – positron pair takes place. The process can occur in the field of a nucleus or of an electron. The threshold for pair production in the electron field is $4m_0c^2$ and is $2\ m_0c^2$ when the process takes place in the nuclear field. The electron and positron can recombine and can annihilate each other. The annihilation is a two photon process producing two photons each having energy m_0c^2. If the secondary photon escapes the true primary absorption cross section σ_a can be expressed as

$$\sigma_a \ = \ \sigma_t \, [\, (E - M_0c^{\,2})/ \, E] \qquad \ldots\ldots\ldots\ldots(2.2)$$

σ_t is the total pair production cross section. The cross section for pair production increases with increasing energy above threshold. In light elements the increase in the pair production is offset by the decrease in Compton cross section over a wide range of energies.

2.4 Elastic scattering

During an elastic scattering event the incident and scattered photons have the same energy except for a negligible loss due to recoil. At the same time the internal energy of the atom does not change. All the constituents of the atom contribute to the elastic scattering of the photon. Rayleigh scattering is due to bound electrons. The

nuclear Thomson scattering and nuclear resonance scattering are the contributions from the nucleus. Vacuum fluctuations in the atomic field constitute Delbruck scattering. To a good approximation scattering amplitude from these processes may be taken as additive and are summed to form the total amplitude. From the analytic properties of scattering amplitude it is found that these processes follow a coherent nature. Moon [1] and Bosch et al. [2] discuss this process in detail.

The incident photon can be absorbed by a bound electron in Rayleigh scattering. The electron then goes to an excited state or into the continuum. When it returns to the original state it emits a photon of the same energy. The photoelectric absorption leading to the intermediate state may be real or virtual. Hence the scattering amplitude is, in general, complex. But for large angles and at high energies the imaginary part is negligible [3]. If the gamma ray energy is about 1 MeV or lower, Rayleigh scattering is the dominant part of elastic scattering from high – Z target at all angles of scattering.

After examining the elastic scattering from lead at an energy 2.76 MeV, Davey [4] observed that at 90^0 and above the amount of scattering exceed the value that would be excepted from Rayleigh scattering alone. This is due to nuclear Thomson scattering which is the low energy limit of photon scattering from the nuclear charge. In the low energy limit the internal charge distribution of the nucleus can be neglected and the scattering is structure independent. The cross section depends only on the atomic number and atomic mass of both scatterer and is independent of gamma ray energy.

The structure dependent part of the nuclear scattering of photons is nuclear Resonance scattering. In this case there is virtual absorption and re – emission of a gamma ray by the nucleus if the gamma ray has the right energy to excite the nucleus from the ground level to a excited level. The cross section for this type of scattering is small if the energy of the photon is far away from excitation energy. In the 1 MeV region the nuclear energy levels are widely spaced and narrow and the photon energy is only rarely close to resonance. Hence from low energy levels resonance scattering contribution is usually negligible. At higher energies the levels are closer and their widths are larger. Hence it is inappropriate to describe excitation in terms of individual level. A strong absorption of photon is observed for many nuclei near gamma energies given by

$$E_0 = \varepsilon \, A \exp(-1/3) \qquad \ldots\ldots\ldots\ldots(2.3)$$

where ε varies between 70 and 80 MeV and A is the atomic number of the element. This scattering is known a Giant Dipole Resonance (GDR) scattering. The GDR is asymmetric and several MeV wide with a low energy tail. Near 1 MeV energies this tail can give contribution to elastic scattering.

The interaction of the electromagnetic field of a photon with the strong Coulomb field of the nucleus give rise to Delbruck scattering and belong to what are known as non linear effects in quantum electrodynamics [5]. In the intermediate state of this process the photon creates a electron – positron pair in the nuclear coulomb field.

Subsequently the pair annihilates and a photon of the primary energy is emitted. The scattering amplitude is complex since the pair creation can be real or virtual. The dissipative part or real part of the amplitude arises from purely virtual intermediate electron state and is thus related to vacuum polarization effects. The absorptive part or imaginary part is associated with the corresponding absorption process namely pair production. The imaginary part is zero below 1.02 MeV because real pairs can be created only above the pair production threshold.

An important factor in the study of scattering is photon polarization. It can be described in terms of two amplitudes denoted by $a^{\parallel}$ and $a^{\perp}$ in linear polarization description. If the incident and scattered photons are polarized in the plane of scattering $a^{\parallel}$ is the amplitude of scattering and if both photons are polarized in plane perpendicular to the scattering plane $a^{\perp}$ is the scattering amplitude. In the circular polarization description the relevant amplitudes are denoted by a^{NSF} and a^{SF}. a^{NSF} corresponds to scattering with no change in circular polarization of the photon(no spin flip) and a^{SF} corresponds to change in polarization(spin flip). The total scattering amplitude can be written as

$$a = a_T + a_R + a_{NR} + a_D \qquad \dots\dots\dots\dots(2.4)$$

since the various elastic scattering processes are coherent in nature. In the present work the energy of interest is less than 1 MeV. Hence nuclear resonance contribution is negligible. Therefore,

$$a = a_T + a_R + a_D \qquad \qquad \ldots\ldots(2.5)$$

In the linear polarization description the total elastic scattering cross section for initially un polarized photon is given by

$$d\sigma/d\omega = r_0^2/2 \left[|a^{\|}_T + a^{\|}_R + a^{\|}_D|^2 + |a^{\perp}_T + a^{\perp}_R + a^{\perp}|^2 \right] \qquad \ldots\ldots(2.6)$$

and

$$d\sigma/d\omega = r_0^2 \left[|a_T^{NSF} + a_R^{NSF} + a_D^{NSF}|^2 + |a_T^{SF} + a_R^{SF} + a_D^{SF}|^2 \right] \qquad \ldots\ldots(2.7)$$

in circular polarization description. A direct measurement of individual contribution is not possible because differential contributions to elastic scattering are indistinguishable as far as the energy of the scattered photon is concerned. Also, there is no secondary process associated with any of the elastic processes which facilitate the detection of that particular process (say, by means of a coincidence experiment).

2.5 Inelastic scattering.

When the photon energy is large compared to the binding energy of an electron, the electron can be considered as free. As in the case of photoelectric effect the incident photon is absorbed and an electron is ejected with a portion of the available energy. A photon of lower energy than the incident photon is created with the division of

energy between the new photon and the ejected electron. Compton [6] derived an expression for energy relation between incident photon and scattered photon treating this process as elastic collision. The energy of the photon scattered at an angle θ is given by

$$E' = E / [1 + \alpha (1 - \cos \theta) \qquad \ldots\ldots\ldots\ldots(2.8)$$

where E' is the energy of the scattered photon, E that of incident photon and $\alpha = E / m_0 c^2$. Fig 2.2 depicts the Compton scattering process.

Because of the assumption of free electron, Compton scattering per electron is independent of Z. The scattering per atom is proportional to Z. With increase in energy Compton scattering decreases much more slowly than photoelectric absorption. This is the most important process from 0.5 to 2.5 MeV range.

The process discussed above is the high energy limit of atomic scattering. A treatment of incoherent scattering from the atom as a whole must consider the binding of electron to atom, their motions and distribution within the atom. During the process, part of the photon momentum is transferred to the electron, which either remains in the excited state or leaves the atom. If the atom is excited to a higher lying bound state the process is called Raman scattering. There is no phase relation between the
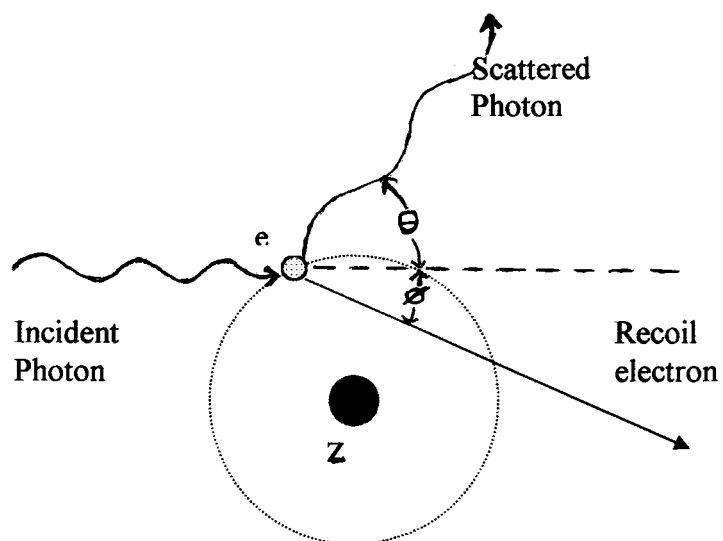
Fig 2.2 Schematic diagram of Compton scattering

scattered radiation in incoherent scattering by different electrons. The total intensity is obtained by adding the intensities due to scattering by each electron of the atom. There is a shift towards longer wave length for scattered photon from bound electron compared to free electron prediction. This is known as Compton defect . Bloch [7] in 1934 showed that in the low energy limit this phenomenon is due to a binding energy effect. Because of the motion of the electrons in the scatterer, the Compton scattered spectrum is Doppler broadened. A Doppler broadened quasi – Compton peak is observed at the free Compton energy. The subject has been reviewed by Cooper [8] and the analysis of broadened line shape of Compton profile gives information of electron momentum distributions.

2.6 Gamma ray attenuation.

2.6.1 Attenuation coefficients

Consider a transmission experiment where mono energetic gamma rays are collimated into a narrow beam and is allowed to strike a detector after passing through an absorber of varying thickness. The transmitted intensity follows an exponential attenuation. Photons are removed from the beam either by absorption or by scattering away from the detector direction. The combined effect of these processes can be characterized by a fixed probability of occurrence per unit length in the absorber. The sum of these probabilities is simply the probability per unit length that the gamma

ray photon is removed from the beam. If μ is used to represent the linear attenuation coefficient then

$$\mu = \tau \text{ (photoelectric)} + \sigma \text{ (Compton)} + \kappa \text{ (Pair production)} \qquad \ldots\ldots(2.9)$$

Here, τ is the photoelectric contribution, σ is the Compton contribution and κ is the contribution from the pair production process. The number of transmitted photons I is then given in terms of I_0, the number without absorber as :

$$I = I_0 \exp (-\mu x) \qquad \ldots\ldots\ldots\ldots\ldots(2.10)$$

The gamma ray photon can be characterized by a mean free path λ defined as the average distance traveled in the absorber before an interaction takes place. Its value can be obtained from

$$\lambda = \int_0^\infty (x\, e^{-\mu x}\, dx) / \int_0^\infty e^{-\mu x}\, dx = 1 / \mu \qquad \ldots\ldots\ldots\ldots(2.11)$$

The typical value of λ range from a few mm to tens of cms in solids for common gamma ray energies. The linear attenuation coefficients vary with the density of the material even through the absorber material is same. Therefore the mass attenuation coefficient is widely used and this quantity is given by μ / ρ.

For a given gamma ray energy the mass attenuation coefficient does not change with the physical state of a given absorber. The mass attenuation coefficient of a compound or mixture of element can be calculated from the mixture rule [9] :

$$(\mu / \rho)_c \;=\; \sum_i W_i \; (\mu / \rho)_i \qquad \ldots\ldots\ldots\ldots\ldots\ldots\ldots(2.12)$$

where W_i represents the weight fraction and $(\mu / \rho)_i$ the mass attenuation coefficient of element i in the compound or mixture.

2.6.2 Absorber mass thickness

If we write the attenuation law for gamma ray in terms of mass attenuation coefficient it takes the form

$$I \;=\; I_0 \exp(-\mu / \rho) \, \rho t \ldots\ldots\ldots\ldots\ldots\ldots\ldots\ldots(2.13)$$

ρt is known as the mass thickness of the absorber that determines the degree of attenuation. The unit is historically mg / cm^2. The thickness of absorber used in radiation measurement is therefore often measured in mass thickness rather than physical thickness.

2.6.3 Good geometry set up for gamma ray attenuation studies.

In gamma ray attenuation measurements, the gamma rays are usually collimated to a narrow beam before striking the absorber [10] and is known as narrow beam or good geometry measurement. In this case only those gamma rays from

the source which escape interaction inside the absorber are counted by the detector. Real measurements are carried out under different circumstances in which good collimation of gamma rays is not always possible. Most types of detectors cannot distinguish between gamma rays that are directly coming from the source and those that are reaching them after being scattered from the absorber. The condition that lead to the simple attenuation is there fore violated in the broad beam or bad geometry measurement because of the additional contribution of the secondary gamma rays. The situation is handled using the equation [11]

$$I / I_O = B(t, E_r) \exp(-\mu t) \qquad \ldots\ldots\ldots\ldots\ldots\ldots(2.14)$$

The factor $B(t, E_r)$ is known as build up factor. The magnitude of the build up factor depends on the type of the gamma ray detector used. The build up factor also depends on the specific geometry of the experiment. In a narrow beam good geometry set up the diameter of the collimation channel and the distance between the absorber and detector are chosen such that the so called in-scattering angle is less than about 0.5^{0} or so.

REFERENCES

1. Moon. P.B, Proc. Phys. Soc. A63(1950)1189

2. Bosch. R. , Lang. J. , Muller. R. and Wolfli. W , Helv. Phys. Acta 36(1963)625

3. Levinger J.S , Phys.Rev.87(1952)656

4. Davey. W.G , Proc. Phy. Soc.66(1953)1059

5. Kane. P.P and Basavaraju .G. , Rev. Mod. Phys. 39(1967)52

6. Compton .A.H. , Phys. Rev. 22 (1923)409

7. Bloch. F. , Phys. Rev.46(1934)674

8. Cooper. M.J. , Rep. Prog. Phys. 48(1985)415

9. R.D. Evans, "The Atomic Nucleus" (McGraw Hill, 1955) p. 713

10. J.H. Hubbel, NSRDS Report – NBS 529 (1969)

11. Glenn F. Knoll, "Radiation Detection and Measurement" 2nd Edn, (1989) John, Wiley & Sons – p. 56

REVIEW OF PHOTON ATTENUATION STUDIES

CHAPTER III

REVIEW OF PHOTON ATTENUATION STUDIES

3.1 Introduction

After the discovery of gamma rays, great attention has been given to study the attenuation of these radiations as they pass through matter. In the earlier days Geiger Muller counters were used as detectors for the gamma rays transmitted through the material. Proportional counters were used in the X – ray region. Later on scintillation and semiconductor detectors were fabricated and were used to study the attenuation effects. These latest detectors give much more accurate measurements. Review of the early investigations have been given by Davisson and Evans [1] .They conducted a detailed theoretical survey of the absorption of radiation in the energy range from 0.1 MeV to 6 MeV. The tabulations of White [2] and White & Grodstein [3] cover the energy range from 10 keV to 100 MeV. Davisson [4] updated these tables using theoretical estimates of atomic photo effect and electron field pair production. Hubbell's compilation [5] in 1969 is based on a new analysis with all available information. Storm and Israel [6] gives a tabulation which is widely used. They list photon cross sections for all elements from Z = 1 to Z = 100 for energies 1 keV to 100 MeV. Plechaty et al [7] have compiled similar data down to 0.1 keV. Hubbell et al [8] compiled tables of photon cross sections for all elements Z = 1 to Z = 100 in the energy range 1 MeV to 100 GeV.

They also list pair and triplet production cross sections and cross sections for atomic photoeffect and coherent and incoherent scattering. Because of uncertainty in the screening and Coulomb corrections to pair production cross section the earlier tabulations were unreliable. The Hubbell's tables use improved form factors in the screening correction and a semi empirical Coulomb correction. Jackson and Hawkes [9] review attenuation coefficients for elements and mixtures and develop parametric fit for the individual collision processes in the energy range 30 – 150 keV. Theoritical values of attenuation coefficients for forty elements starting from Z = 1 to Z = 92 are tabulated by Hubbell [10]. Experimental data contained in the National Bureau of Standards collection of measured X – ray attenuation data and cross section calculated using a relativistic Hartree –Slater model for the photoelectric cross section for all elements Z = 1 to Z = 92 are collected by Saloman et al [11]. They also show the cross sections obtained using the semi empirical set of recommended values of Henke et al. [12].

Interpolation formula have been suggested by Mc Master et al [13] in the energy range 1keV to 1 MeV. Other authors [14] also have suggested analytical fits for purposes of interpolation. The typical accuracy of the theoretical compilations lies in the range of 1 – 10 % depending on the atomic number of the absorber and the X – ray or gamma ray energy. The analytical interpolation formulae have accuracies of 1 – 2 % with respect to the compiled theoretical data.

A more recent compilation of X- and gamma ray attenuation coefficients is the work of Berger and Hubbell (XCOM) [15].

3.2 Review of various experimental studies

Some of the recent experimental studies are reviewed below.

Mc Crary et al. [16] measured attenuation coefficients for several elements using X – rays having energies between 25 and 130 keV. Conner et a. [17] measured the coefficients for energy range up to 2.75 MeV for elements with atomic number ranging from 4 to 94. Gopal and Sanjeevaiah [18] carried out similar studies for C , Al , Cu , Sn , and Pb for energies between 84 and 661.6 keV. Earlier experiments using Sodium Iodide detectors are described by Conner et al. [17] and also by Goswami and Chaudhury [19]. The letter authors minimized multiple scattering from the sample by ensuring that the FWHM of the gamma ray photo peak with attenuator is almost the same as that with out the attenuator in position. It is found that only a few systematic studies of attenuation coefficients with high resolution Ge(Li) detectors were reported [20 – 23]. Christmas [21] demonstrated that attenuation coefficient measurement with high level of accuracy even in wide beam is possible using Ge(Li) detectors. Nuclear resonance scattering has been made use of [24] in determining attenuation coefficients for gamma rays in 6 – 8 MeV range with an effective resolution of about 20eV. A 30 MeV synchrotron provided the source of photons in an absorption experiment [25] with high Z elements in the range 7 – 20 MeV.

On the low energy side there has been several attenuation measurements [16, 26 - 29] on X – rays. Some of the workers used radio active X –ray sources while others have used characteristic X - rays as well as bremsstrahlung from X – ray machines. Gowda and Powers [30] used K_α and L_α X – ray lines produced by heavy ion interaction with thick targets of different materials as the source.

Gopal and Sanjeeviah [18] have demonstrated the effect of multiple scattering for μt varying up to 4.2 for 84 and 661.6 keV gamma rays using carbon and lead absorbers. In their experiment using sodium iodide detector, they observed a deterioration of the resolution of the detector as the absorber thickness increases above $(1/\mu)$, with a simultaneous increase in the value of the measured attenuation coefficient.

Kane et al. [31] conducted attenuation coefficient measurement for lead , tantalum and molybdenum for 661.6 keV and 1116 keV gamma rays. The attenuation coefficient for lead were also measured at 1.17 MeV and 1.33 MeV. Their experimental values were in fair agreement with the calculated ones. They used a Ge(Li) detector and a narrow beam geometry. The effect of multiple scattering on the pulse height distribution of the transmitted gamma rays and on the measured attenuation coefficients were studied and shown to be small up to three mean paths.

Varier et al. [32] conducted a study of the effect of transverse dimensions, that is, in a direction perpendicular to the direction of the incident beam. They concluded that for small transverse dimensions , absorber thickness up to even four mean paths does not

significantly contribute to multiple scattering. For larger transverse dimensions , multiple scattering is important and could affect the measured attenuation coefficient for absorber thickness above one mean free path. The criterion $\mu t < 1$ could also apply for transverse dimensions also. Kerur et al. [33] employed a new method for determining the mass attenuation coefficient for X – rays incorporating the suggestion of Creagh and Hubbell [34] to minimize small angle scattering and multiple scattering.

In many of the attenuation coefficient measurements the aim is to determine the total photoelectric cross sections by subtracting the other theoretically calculated partial cross sections from the total gamma ray cross section .

By applying the mixture rule , from the measured attenuation coefficients of the compounds , the corresponding value for the constituent element can be obtained. Milller and Greening [29] measured the mass attenuation coefficient for elements with Z = 1 to Z = 18 to an over all accuracy of 1%. They used the compounds C_2H_4 , CO_2 , CF_4 , H_2S ,HCl, SiO_2 , $(C_2H_5)_3PO_4$, air and gaseous elements N_2 , O_2 , Ne , Ar , Mg , Al at a series of energies from 4.508 keV to 25.192 keV. From the results of the above study performed using a narrow beam geometry and homogeneous absorbers , the authors deduced a set of values of total attenuation cross sections and photoelectric cross sections for elements with Z in the above range.

The whole atom integral incoherent scattering cross sections have been obtained from the total attenuation cross section by studies conducted by Umesh et al. [35] in elements with atomic numbers ranging from 1 to 56 at photon energies of 279.8 , 514 , 661.6 , and 1115.5 keV. The total attenuation cross sections were derived with the aid of mixture rule from total attenuation cross sections in 26 solid chemical compounds (like MgO, NaF , NaCl, KCl,CuO, KBr, KI, BaO etc) measured by performing transmission experiments in good geometry set up. The values of the whole atom integral incoherent scattering cross sections have been compared with the Klein – Nishina cross sections, self consistent HF values of Hubbell et al and earlier experimental results. Electron binding effects were also discussed. The integral incoherent scattering cross sections were also obtained from the total attenuation cross sections in the elements La, Ce, Pr, Nd, Sm, Gd, Dy, Ho, Er, Pb, Ta and Bi obtained from measurements on their compounds at the photon energies listed above by Umesh et al. [36]

Umesh et a.l in the above experiment used in addition to the subtraction method another technique to derive the incoherent scattering cross section. The main mode of gamma interaction in low Z material in the chosen energy region is incoherent scattering. Hence the linear portion of the μ vs Z curve can be strictly attributed to incoherent scattering only. The initial linear portion , fitted to a straight line and extrapolated, gives the individual incoherent scattering cross section. The mixture rule and extrapolation method were also used to find integral incoherent scattering cross section of ^{60}Co gamma rays in 38 elements from the measured total attenuation cross section of their compounds by Umesh et al. [37]. They also studied in coherent scattering cross section

of some rare earths elements for [203]Hg gamma rays by subtracting Scofields photo effect and experimental incoherent scattering cross sections from the total attenuation cross section [38].

The method of estimating incoherent scattering cross section from total attenuation measurement was also tried by Roy [39]. He comments on the relativistic form factor to estimate the contribution of coherent scattering of photons and its subsequent use for the evaluation of incoherent scattering cross section from the measured total photon cross section

The method of subtracting other partial cross sections from the total cross sections has been applied by Sharma , Mudhahar , Singh , Sahota [40,41] to determine pair production cross section at 1.16, 1.598, and 2.754 MeV for Cu and Sn and at 2.754 MeV for elements with atomic numbers between 6 and 72. Sherman and Ewart [42,43] have also conducted experiments to measure total photon absorption cross section and pair production cross section from them.

Now synchrotron radiation is available and studies based on it established the fact that photon absorption coefficients show oscillatory behavior near edges. It has been interpreted in terms of local electronic and structural properties around the absorbing atom [44]. In a study of total photon cross section in KBr , RbBr and CsBr at 10.676 , 13.93 14.413 , 26.345 and 59.357 keV, Lakshminarayna et al. [45] observe 3 to 9% deviation from theory at energies close to absorption edge of bromine. It indicates

sizeable chemical effects in photon interaction and the inapplicability of the mixture rule close to edges. Analysis of data on absolute X – ray attenuation cross section of Krypton in the vicinity of K edge by Deutsch and Hart [46] supports decisive rule of relaxation and overlap effects in determining the shape of the cross section immediately above threshold. Parthasaradhi et al. [47] reported the above photon absorption spectra at the K edge of Ti and Ni and the L_3 edge of Pt and Au recorded using synchrotron radiation. Average photon cross sections at the L_3 edges of Pt and Au are found to be in good agreement with the theoretical data of Scofield.

Singh et al. [48] employed a transmission method for the direct measurement of the energy absorption coefficient of different soil samples by placing a point source of ^{137}Cs inside a spherical shell. Transmitted and scattered gamma rays are detected using a proportional response NaI detector. The measured values are compared with the theoretical values and found in good agreement.

A simple and direct method has been proposed by Jahagirdar et al. [49,50] to obtain fairly accurate total atomic photoelectric cross section by measuring the K X – ray fluorescence spectrum by 123.6 keV gamma ray for elements in the region $42 < z < 82$ by employing a NaI(Tl) spectrometer system in 2π geometry system. The total mass attenuation coefficient of the exciting radiation the total mass attenuation coefficient of k x – ray in the same target and from them the total scattering cross section of the primary radiation have been determined and found in good agreement with theoretical values. Gerward [51] presents the current state of knowledge of X – ray attenuation coefficients

in photon energy range 1 – 100 keV. Jahagirdar et al. [52] conducted the measurement of narrow beam attenuation coefficients using broad beam Geometry Configuration for 145.4 keV photons. They observed that for high Z compounds at 145.4 keV energy, the exponential law of attenuation will be valid even for a broad beam geometry configuration in the transmission range from 50 to 20%.They found the validity of the mixture rule in the above region of transmission.

Nair et al. [53] carried out studies to determine total attenuation cross sections of amino acids at 661.6 keV, 1173 keV and 1332.5 keV. The values are compared with the values calculated with the aid of mixture rule from the data of Hubbell for the individual elements.

Angelone et al. [54] conducted measurement of mass attenuation coefficient for elemental materials in the range 6< Z< 82 using X – rays from 13 up to 50 keV.the mass attenuation coefficients for 22 high purity elemental material(C, Al, Ti etc) were measured in the X –ray energy from 13 to 50 keV using a high purity germanium detector with thin (50 μm) Be window and a variable energy X –ray source. The measured values are compared with the theoretical ones obtained using the XCOM code [15] as well as with other experimental data showing a general agreement .

3.3 Studies on effective atomic numbers via attenuation measurements

The concept of Z dependence of photon interaction has many applications in radiation studies and other fields involving radiation transport through materials. The

effective atomic number has proved to be a convenient parameter for interpreting the gamma ray attenuation by a given medium. Some of the recent studies involving effective atomic numbers are reviewed below.

The total attenuation cross sections in four alloys, telphy, dilver p, anhyster DS , and anhyster M have been measured by Suresh Babu et al. [48] at 32.1, 52, 72.1, 84.3, 145.3, 279.2, and 661.6keV photon energies in a good geometry set up using two NaI(Tl) scintillation detectors for low and medium energy photons. Experimental attenuation cross sections are compared with the theoretical values of Strom and Israel [6] and found to be with in experimental error. The effective atomic number for photoelectric and total gamma – ray interaction are derived and their variation with energy is discussed by them. Mudahar et al. [49] investigated the variation of effective atomic number (Z_{eff}) of certain alloys with photon energy. The effective atomic number of eight alloys (tungsten steel, monel steel, Solder etc) have been studied for the total and partial photon interaction processes over a wide energy range from 10 keV to 100 GeV using theoretical compilation by Berger and Hubbell [15]. The maximum and minimum values of Z_{eff} is at different energies for different alloys depending upon the relative proportion and the range of atomic numbers of constituent elements of the alloy.

Rao et al. [55] studied effective atomic numbers of certain alloys and compounds. They confirmed that Zeff of a material cannot be expressed by a single number, as it is composed of number of elements and the contribution due to each interaction processes is to be accounted for differently. Lingam et al. [56] studied the

total gamma ray cross sections and effective atomic numbers in compounds in the energy region 32 – 662 keV.

Bandal and Singh [57] conducted total and partial mass attenuation coefficients and effective atomic number studies in different solid state nuclear track detectors in the energy range 1 keV to 100 GeV and found that the calculated mass attenuation coefficients and effective atomic numbers are found to vary with the type of interaction of photons with it and the influence of chemical composition Kirankumar and Venkata Reddy [58] studied effective atomic number for materials of dosimetric interest in the energy region 1 keV to 20 MeV for elements Z = 1 to Z= 92. The variation of Z_{eff} values with energy is also discussed. Murthy et al. [59] conducted studies on Z –dependence of photon on simulated materials. The Z dependence of photon cross section and the variation of Z exponents with energy and elemental composition have been studied with emphasis on tissue – equivalent materials. The validity of the evaluated Z – exponents and effective atomic numbers have been tested by means of measured attenuation coefficients in simulated materials in the energy range 13 to 60 keV.

Murthy et al. [60] conducted effective atomic number studies for W/Cu alloys using transmission experiments and verified the validity of the mixture rule. The transmission experiments were conducted in a narrow beam geometry for the photon energy range 60 to 400 keV. Nayak et al. [61] conducted studies on effective atomic number of some polymer and other materials for photoelectric process at 59.54 keV from the accurately measured total attenuation coefficients.

More recently, Shivaramu et al. [62 - 64] conducted studies on effective atomic numbers for photon energy absorption and effective atomic numbers for photon interaction of some low – Z substances of dosimetric interest such as A – 150 tissue equivalent plastic (A150 TEP) in the energy region 1 keV to 20 MeV. The effect of absorption edges on effective atomic numbers and their variation with photon energy and the possibility of defining two sets of values of effective atomic numbers below the absorption edges of elements present in the composite substance are discussed by the authors in the article.

Regarding the experimental investigations on absorbers for which the attenuation change with time, no previous reported works has come to the author's notice till date.

REFERENCES

1. Davisson C.M and Evans R.D, Rev. Mod. Phys., 24 (1952) 79

2. White G.R, NBS Report No 1003 (1952)

3. White-Grodstein G., NBS Circular No. 583 (1957)

4. Davisson C.M. , Alpha Beta and Gamma ray spectroscopy Vol I, North Holland, Amsterdam (1965) 827

5. Hubbell J.H., Report NSRDS-NBS 529 (1969)

6. Storm E. and Israel H.I., Nuc. Data Tables A7 (1970) 565

7. Plechaty E.F., Cullen D.E. and Howerton R.J., Report UCRL – 50400, Vol. 5, rev. 3 (1981)

8. Hubbell J.H., Gimm H.A. and Overbo I., J. Phys. Chem. Ref. Data 9 (1980) 1023

9. Jackson D.F. and Hawkes D.J., Phys. Rep. 70 (1981) 169

10. Hubbell J.H., Int. J. Appl. Radiat. Isot. 33 (1982) 1269

11. Saloman E.B., Hubbell J.H. and Scofield J.H., At. Data Nucl. Data Tables 38 (1988) 1

12. Henke B.L., Lee P., Tanaka T.J., Shimabukuro R.L. and Fujikawa B.K., At. Data Nucl. Data Tables 27 (1982) 1

13. McMaster W.H., Grande N.K.D., Mallet J.H. and Hubbell J.H., UCRL Report No 50174 –SEC ZR-1 (1969)

14. Hsu H.H. and Dowdy E.J., Nucl. Inst. Meth. 204 (1983) 505

15. Berger M.J. and Hubbell J.H., XCOM : Photon Cross sections on a Personal Computer, NBSIR 87 – 3597 (1987)

16. McCrary J.H., Plassmann E.H., Puckett J.M. Conner A.L. and Zimmermann E.W., Phys. Rev. 153 (1967) 307

17. Conner A.L., Atwater H.F., Plassmann E.H. and McCrary J.H., Phy. Rev. A1 (1970) 539

18. Gopal S. and Sanjeevaiah B., Nucl. Inst. Meth. 107 (1973) 221; Phys. Rev. A8 (1973) 2814

19. Goswami B. and Chaudhuri N., Phys. Rev. A 7 (1973) 1912

20. Henry L.C. and Kennett T.J., Can. J. Phys. 49 (1971) 1167

21. Christmas P., Int. J. Appl. Radiat. Isot. 25 (1974) 25

22. Hansen H.H. and Parthasaradhi K., Z. Phys. A277 (1976) 331

23. Kane P.P., Basavaraju G. and Varier K.M., Nucl. Inst. Meth. 147 (1977) 507

24. Moreh R. and Wand Y., Nucl. Phys. A252 (1975) 423

25. Gurevich G.M., Lazareva L.E., Mazur V.M. and Mekulov S. Yu. And Solodukhov G.V., Nucl. Phys. A338 (1980) 97

26. Prasad R., Phys. Rev. A18 (1978) 2167

27. Parthasaradhi K. and Hansen H.H., Phys. Rev. A10 (1974) 563

28. Heinrich K.F.J., "Electron Probe", Wiley, New York (1966) 296

29. Miller R.H. and Greening J.R., J. Phys. A7 (1974) 2332; A7 (1974) 2345

30. Gowda. R and Powers. D, Phys. Rev. A 32 (1985) 2637

31. Kane. P.P, Basavaraju. G and Varier. K.M , Nucl.Instrum.Meth.147 (1977) 507

32. Varier. K.M , Nasirudden Kunju. S and Madhusudanan . K , Phys.Rev .A 33 (1986) 2378

33. Kerur B.R , Thontadarya .S.R and Hanumaiah .B , Appl.Radiat.Isot.42 (1991) 571

34. Creagh. D.C and Hubbell. J.H , Acta Crystallogr.A43 (1987) 102

35. Umesh T.K , Ranganathaiah C, Ramakrishna Gowda , Puttaswamy K.S and Sanjeevaiah .B ,Phys.Rev.A 23 (1981) 2365

36. Umesh .T.K , Ramakrishna Gowda and Sanjeevaiah .B , Phys.Rev. A25 (1982) 1986

37. Umesh .T.K , Ranganathaiah.C and Sanjeeviah .B ,Phys Rev.A29(1984)387

38. Umesh.T.K , Ranganathaih .C and Sanjeeviah .B , Ind.J.Phys.58a(1984)368

39. Roy. S.C. , Phys.Rev. A 27 (1983)1685

40. Shrma. R.K , Mudahar G.S , Singh.K and Sahota .H.S Ind. J. Phys. 57A (1983) 302

41. Mudahar .G.S. , Sharma .R.K , and Sahota .H.S . Ind. J. Phys 59A (1985) 92

42. Sherman .N.K. and Ewart .G.M. , Can. J. Phys. 59 (1981) 914

43. Sherman .N.K. and Ewart . G.M. ,Phys rev.C.27 (1983) 1011

44. Lee .P.A. , Citrin .P.h , Eisenberger .P and Kincaid .B.M , Rev. Mod. Phys. 53 (1981) 769

45. Lakshminarayana .V , Tan. A.T.L , Giles .I.S and Rajaratnam .A. Nuovo Cimento 91A (1986) 331

46. Deutsch .M and Hart .M , J. Phys. B 19 (1986) L303

47. Parthasaradhi .K , Esposito .a , Mobilio.S and Pelliccioni .M , M. Phys. Rev . A38 (1988) 1608

48. Singh. K , Bal. H.K , Sohal. I.K ana Sud. S.P. Appl. Radiat. Isot. Vol 42 (1991) 1239

49. Jahangirdar. H.A , Hanumaiah. B. , Thontadarya. S.R . Appl. Radiat. Isot. Vol 43 (1992) 399

50. Jhangiridhar. H.A , Hanumaiah. B , Thontadarya. S.R. , Appl. Radiat. Isot. Vol 43 (1992) 783

51. Gerward. L., Radiat. Phys .Chem .Vol 45 (1993) 783

52. Jahangirdar. H.A , Hanumaiah. B. , Thontadarya. S.R . Appl. Radiat. Isot. Vol 44 (1993) 1248

53. Gopinathan Nair. K.P . Umesh. T.K and Ramakrishna Gowda., Radiat . Phys . Chem.Vol.45 (1995) 231

54. Angelone. M , Bubba. T and Esposito. A. Appl. Radiat. and Isot. 55 (2001) 505

55. Rao J.R., Lahshminarayan V. and Jnananda S., J. Sci. Indust. Res. 20B (1961) 587

56. Lingam S.C., Basu K.S. and Reddy D.V.K., Ind. J. Phys. 58A (1984) 285

57. Bhandal G.S. and Singh K., Rad. Phys. Chem. 47 (1994) 109

58. Kiran Kumar T and Reddy K.V., Rad. Phys. Chem. 50 (1997) 545

59. Murthy C.R, Rao A.S.N and Rao G.K, App. Rad. Isot. 51 (1999) 335

60. Murthy V.R.K, Winkoum D.P. and Devan K.R.S., App. Rad. Isot. 53 (2000) 945

61. Nayak G.N., Vijaya M.G. and Siddappa K., Rad. Phys. Chem. 61 (2001) 559

62. Shivaramu, Vijayakumar R. Rajasekharan L. and Ramamurthy N., Rad. Phys. Chem. 62 (2001) 371

63. Shivaramu, Amutha R. and Ramprasath V., Nucl. Sci. Eng. 132 (1999) 148

64. Shivaramu and Ramprasath V., Nucl. Inst. Meth., B168 (2001) 294

PRELIMINARY MEASUREMENTS ON GAMMA ATTENUATION IN NARROW BEAM AND BROAD BEAM GEOMETRIES

CHAPTER IV

PRELIMINARY MEASUREMENTS ON GAMMA ATTENUATION IN

NARROW BEAM AND BROAD BEAM GEOMETRIES

4.1 Introduction

In order to determine experimentally accurate values for the attenuation coefficients for gamma rays using a transmission setup, it is necessary that the detector should detect only those gamma rays which are transmitted through the absorber without undergoing any interaction in the medium. Consequently, one should ensure that gamma rays which are scattered at any angle, however small, should not be allowed to fall on the detector. The geometrical arrangement should include sufficient collimation for the incident as well as the transmitted gamma ray beams. Such an arrangement is referred to as the narrow beam good geometry set up. As a general convention, such a set up will ensure that scattered gamma rays outside a cone of half angle of 0.5° are not falling on the detector.

In an actual experimental situation, it may not always be possible to ensure a perfect narrow beam setup. In this case, gamma rays which are scattered through small angles may fall on the detector and get detected along with the transmitted ones. Such an

arrangement is called a poor geometry (broad beam) setup. Corrections should be applied to the measured attenuation coefficients for the so called "in-scattering".

Some preliminary investigations have been performed as part of the present thesis work to study the effect of broad beam geometry on the measured coefficients. The following sections give the details of the set up and measurements and the results obtained.

4.2 Experimental details

A 0.5 mCi ^{137}Cs source has been used in the present studies. It has been procured from the Bhabha Atomic Research Centre, Mumbai. It was well shielded by means of lead bricks. For the narrow beam setup, the gamma ray beam from the source was collimated by using a cylindrical lead block with a central hole of diameter 1 cm. The transmitted beam was also collimated using a similar lead cylinder. The absorbers used were lead sheets of dimensions 5 cm x 5 cm and had thickness of 0.9 gm / cm2. Figures 4.1 and 4.2 provide schematic diagrams of the two experimental setups. The large in-scattering angle θ is indicated in fig 4.2.

The detector was a 1 3/4" X 2 " NaI(Tl) detector, coupled to a ten dynode photomultiplier tube in an integral assembly, supplied by ECIL, Hyderabad. The detector bias was given from an ECIL HV bias supply. The output pulses from the PMT anode were fed to the main Linear Amplifier through a pre amplifier. Spectra were recorded

using a Nucleonix 4K MCA, for various absorber thicknesses. The spectra were divided into a number of energy bins, each bin covering 50 channels (corresponding to about 45 keV), starting at around 200 keV. The total counts in the various energy bins were determined and plotted on a semi logarithmic plot as a function of absorber thickness. The slopes of the resulting straight lines were evaluated by a linear least squares procedure.

4.3 Results and Discussions

The semi logarithmic plots of the counts per bin are given in figures 4.3 and 4.4 for the narrow beam and broad beam setups respectively. The straight lines are the least squares fits through the experimental points. The overall linearity of the plots is good for all the energy bins.

The value of the attenuation coefficient for the 662 keV gamma rays used in the present investigations have been evaluated using the slope of the plots in fig 4.3 for the photo peak (highest energy bin) for the narrow beam geometry. This value is 0.103 cm^2 / gm. This compares excellently well with the theoretical value of 0.101 cm^2 / gm obtained from the XCOM package [1]. In contrast to this, the corresponding coefficient derived from the photo peak data for the broad beam geometry (using the slope of the plots in fig 4.4 for the photo peak) is 0.078 cm^2 / gm, which is smaller than the narrow beam value by about 24 %. The extra intensity of the detected gamma beam which accounts for this difference is obviously attributable to the in-scattering.

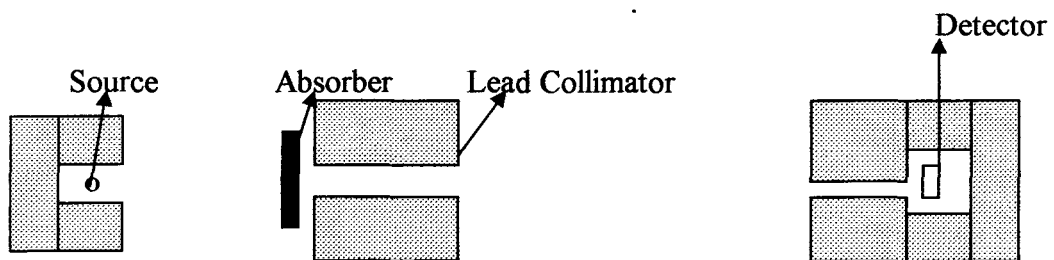Source   Absorber   Lead Collimator   Detector

Fig. 4.1 Schematic diagram of the experimental setup for narrow beam geometry
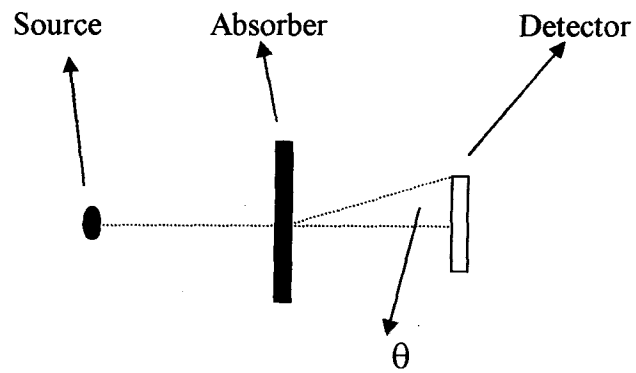
Gamma attenuation measurements

Fig. 4.2 Schematic diagram of the experimental setup for broad beam geometry
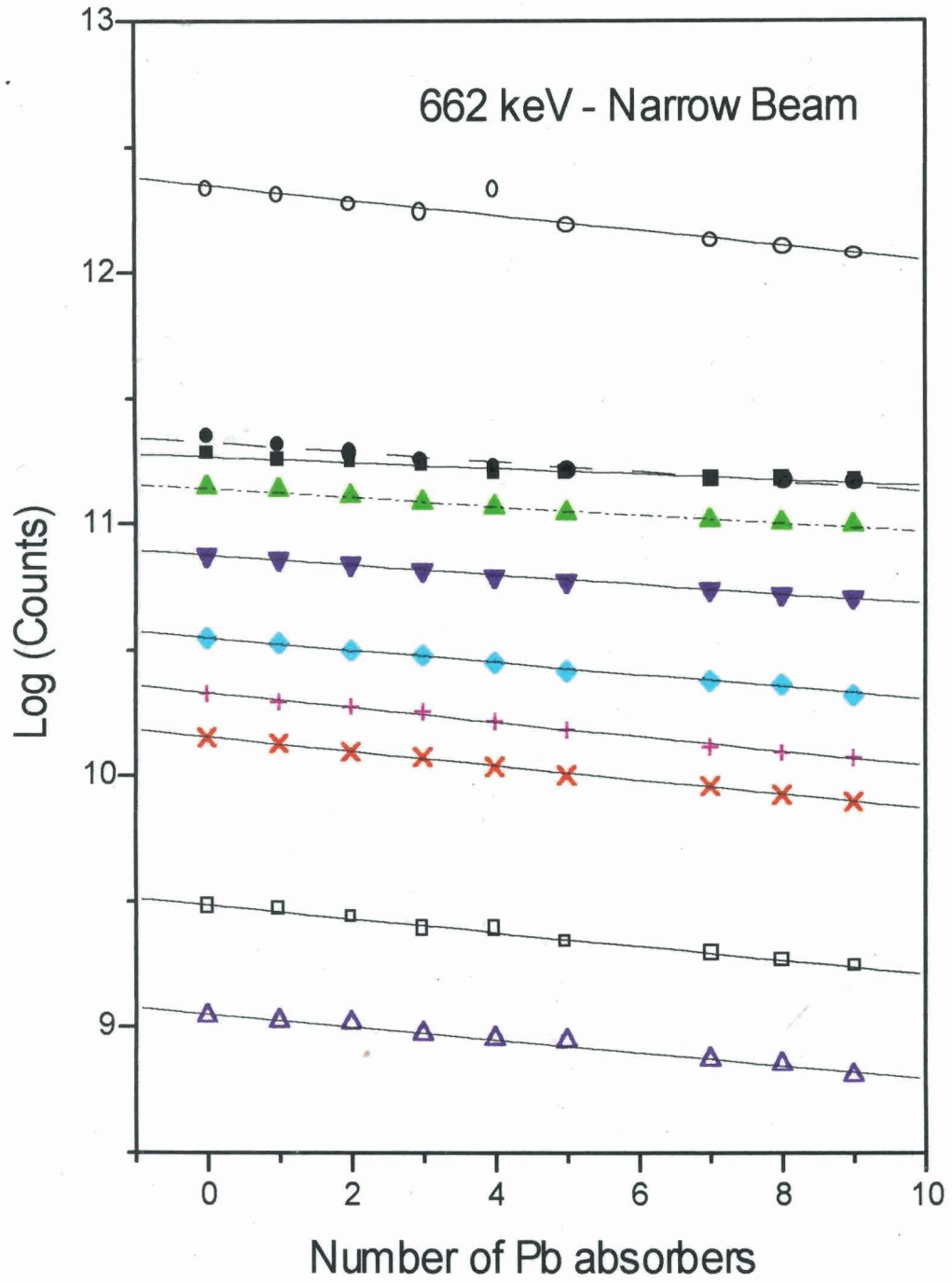Gamma attenuation measurements

Fig. 4.3 - Semilog plots of the transmitted intensity as a function of Pb absorber thickness
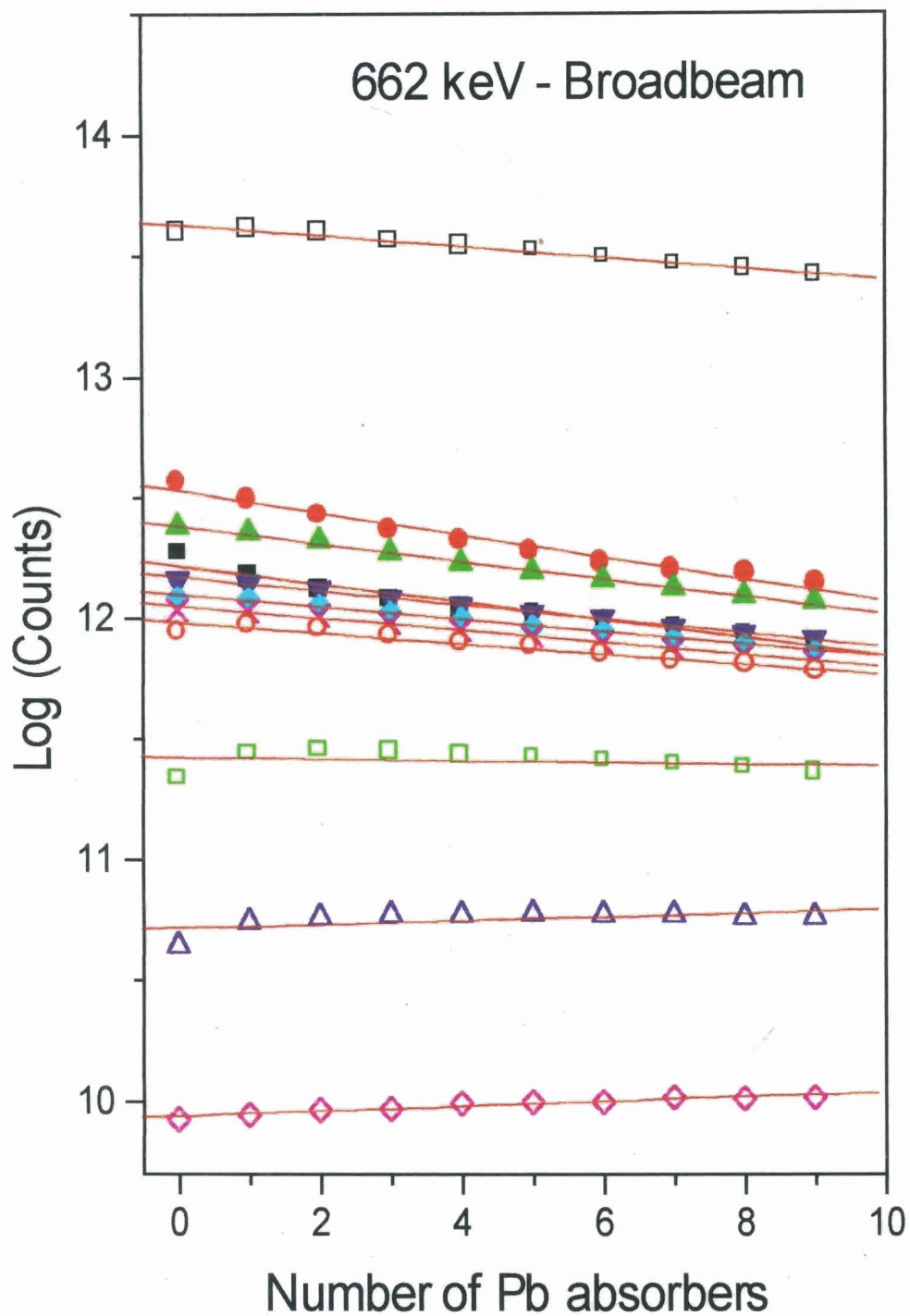
Fig. 4.4 - Semilog plots of transmitted intensity as a function of Pb absorber thickness

The slopes of the linear fits in the above figures have been plotted in figure 4.5 for the two geometries for the different energy bins of the spectrum. It is worth noting that the magnitude of the slope is different for the different energy bins and also for the different geometries. Especially, it is interesting to note that for the energy bin of about 540 keV, the slope is of opposite sign in the broad beam plot. Moreover above about 350 keV, the slopes of the plots is smaller for the broad beam geometry. This is a clear-cut manifestation of the build up factor. Below 350 keV, the slopes are smaller for the narrow beam geometry.

REFERENCES

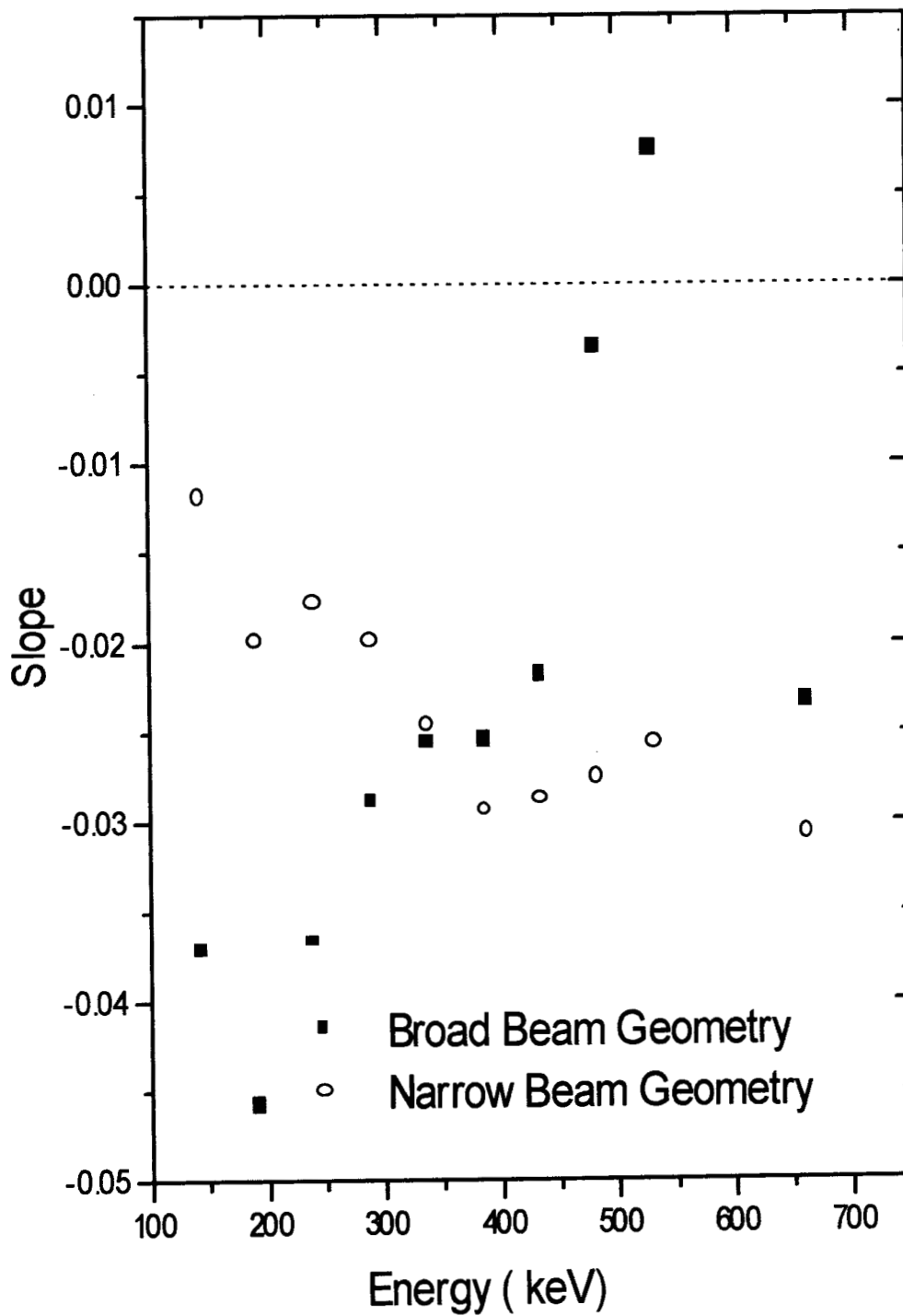1. M.J. Berger and J.H. Hubbell, NIST Standard Reference Data Base (1990)

Fig. 4.5 Variation of slope of semilog plots of transmitted intensity vs. thickness

EFFECT OF ABSORBER POSITION ON GAMMA RAY SPECTRA

CHAPTER V

EFFECT OF ABSORBER POSITION ON GAMMA RAY SPECTRA

5.1 Introduction

In experiments involving measurement of gamma ray spectra under different conditions it may be required to use suitable absorbers in between source and detector. Unless a very narrow beam good geometry setup is used in the measurements forward inelastic scattering of the gamma rays from the absorber will lead to a distortion in the lower energy part of the pulse height spectrum of the gamma rays [1]. Since the maximum angle of scattering depends on the position of the absorber in between the source and the detector, the overall shape of the spectrum in turn depends on the absorber position. As a result, in cases where many gamma energies are involved, it becomes difficult to evaluate the spectral components due to the individual gamma energies.

We have studied the pulse height distribution of ^{137}Cs gamma rays passing through lead absorbers as a function of absorber position. Some preliminary results were presented at the National Radiation Physics Symposium at Mangalore in 1999 [2]. The details of the experiment and the results are presented below.
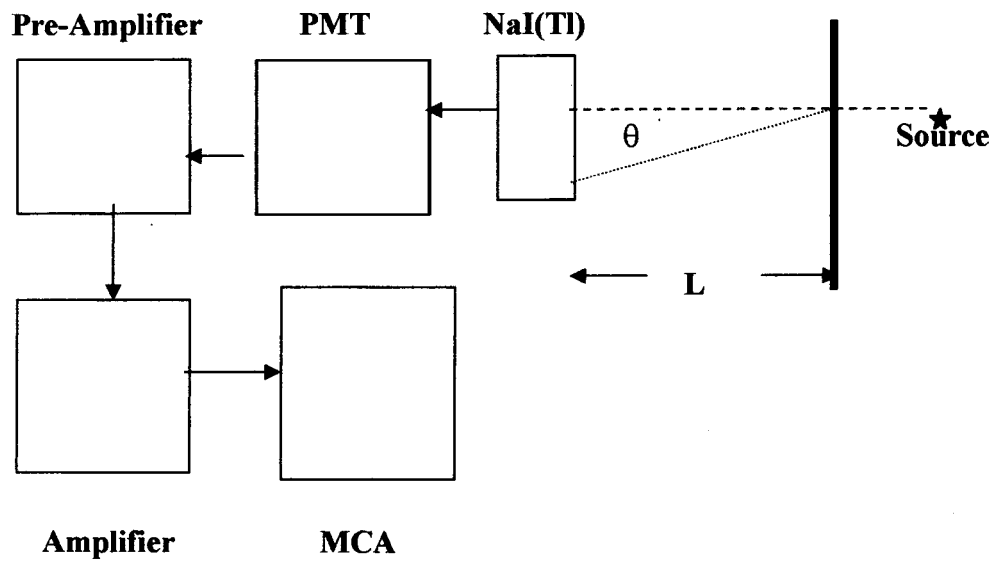
Figure 5.1 Experimental set up

5.2 Experimental Method

A 1 μCi ^{137}Cs source procured from BARC, Mumbai has been used in the present investigations to provide gamma rays of 662 keV energy. A 1 ¾" X 2" Sodium iodide detector was used for detecting the gamma rays. Standard NIM setup was used to store the pulse height spectrum of the detected gamma rays on a Nucleonix 4K Multichannel Analyzer. A poor geometry broad beam set up was assembled. Lead absorbers in the form of square sheets of dimensions 8 cm X 8 cm X 0.3 mm were used. The absorbers were placed vertically in between the source and the detector at distances of 0 cm, 5cm, 10 cm and 15 cm from the detector face. At each position data were taken without any absorber and for three values of the absorber thickness (3 sheets, 6 sheets and 9 sheets). A schematic diagram of the setup is given in fig. 5.1. Fig. 5.1 also shows the maximum angle at which the gamma rays scattered from the absorber can still reach the detector and be detected.

Spectra were collected in the MCA to achieve good statistical accuracy. The counts in the channels were plotted for each absorber position and for each absorber thickness, after normalization to the photo peak counts.

5.3 Results and Discussions

Figures 5.2 – 5.5 show the normalized spectra in the energy region 220 keV to 580 keV for the four absorber positions. Each figure contains the spectra for the four absorber
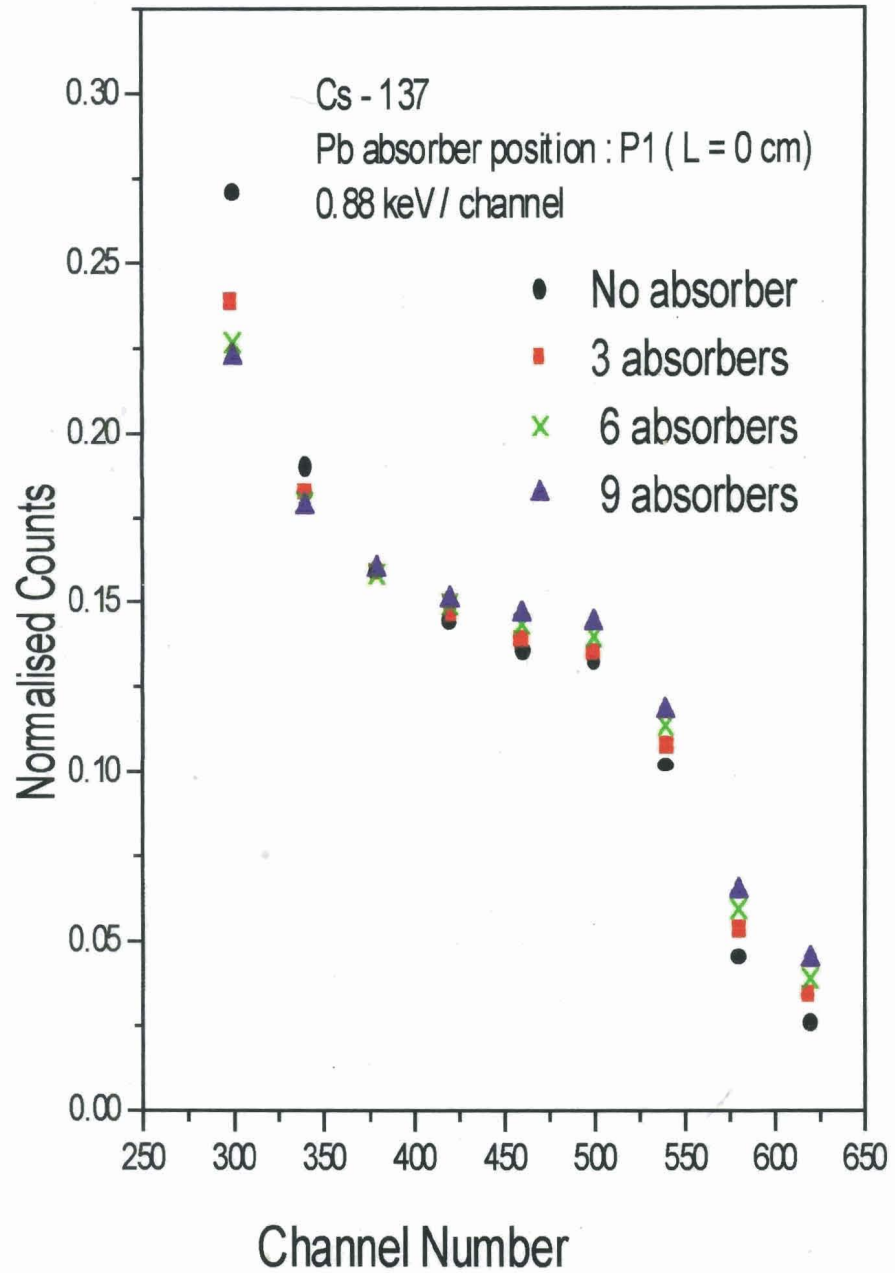
Figure 5.2 Normalized spectra with Pb absorber at position 1 for various absorbers thickness

Cs - 137
Pb absorber position : P2
0.88 keV / channel

- No absorber
- 3 absorbers
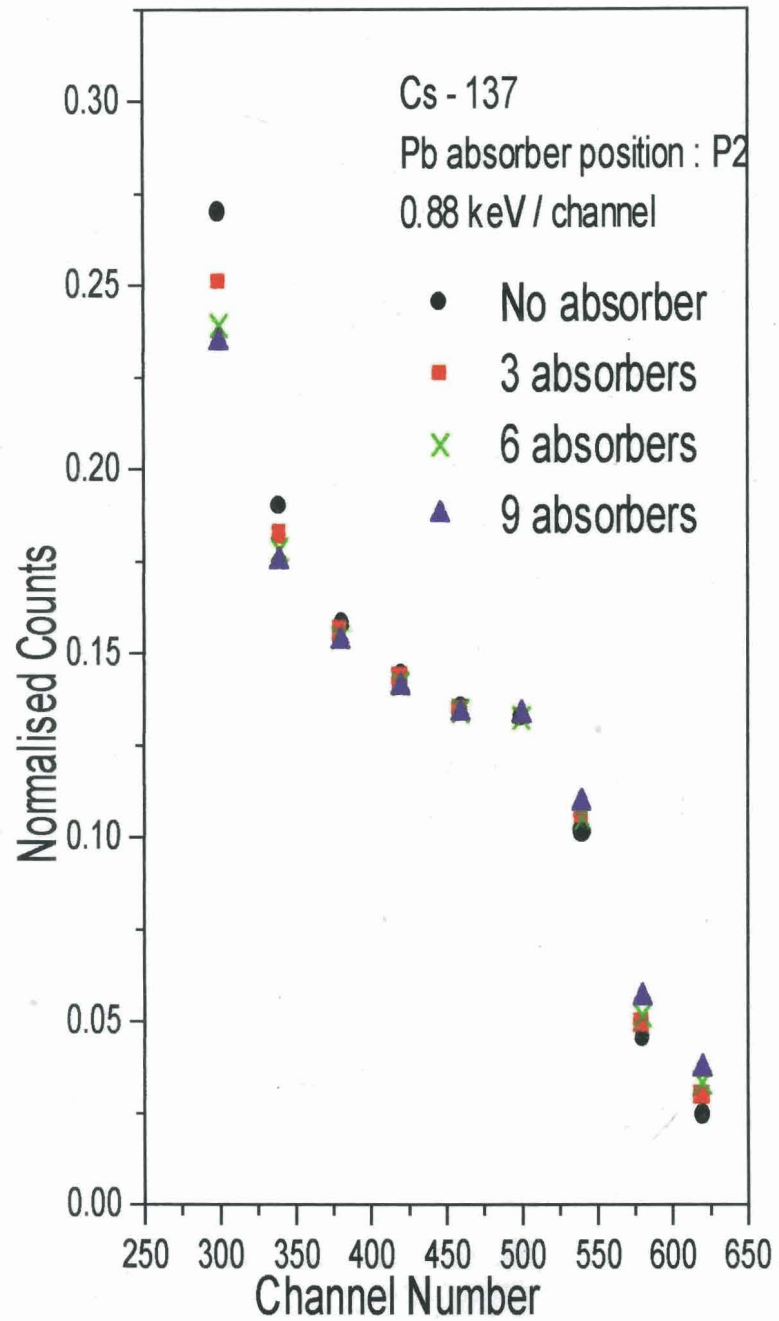- 6 absorbers
- 9 absorbers

Fig 5.3 Normalized spectra of transmitted gamma
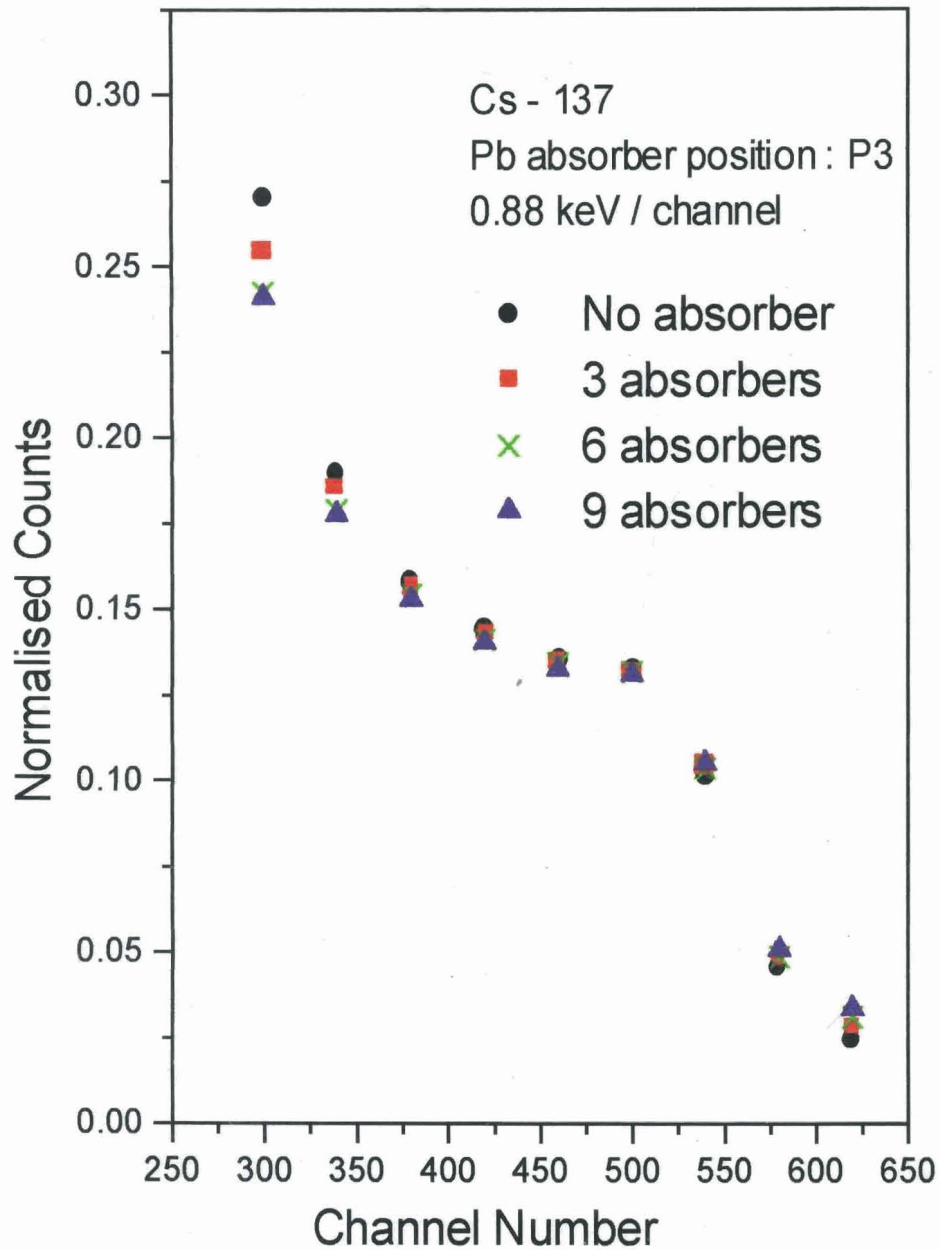rays for Pb absorber position 2 for various absorber thickness

Fig 5.4 Normalized spectra of transmitted gamma rays
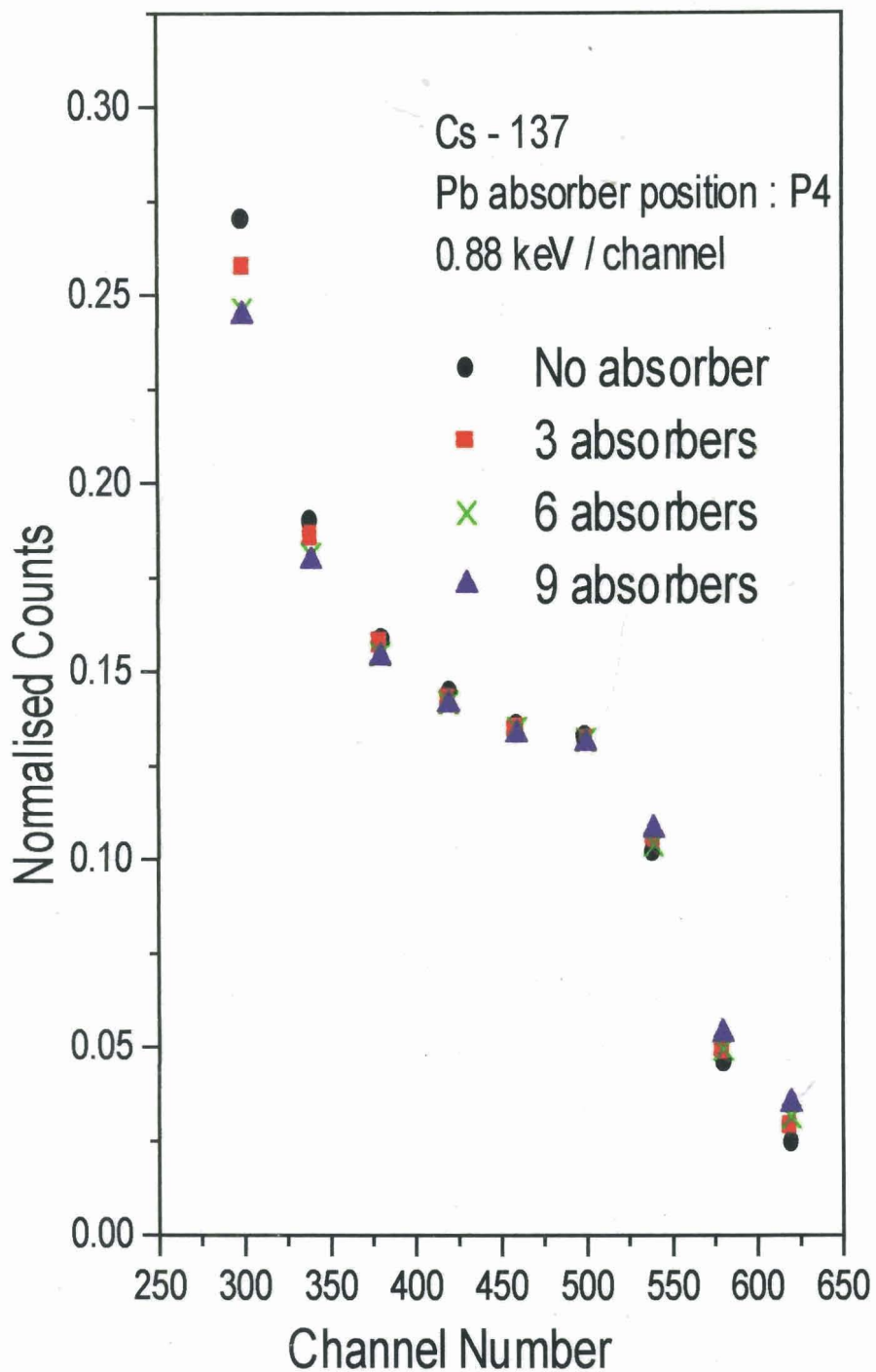at Pb abosrber position 3 vs. absorber thickness

Fig 5.5 Normalized spectra of transmitted gamma rays for various absorber thicknesses at Pb asorber position 4

thicknesses used. One important feature of these spectra is the expected non-overlapping of the spectra, arising from the contribution of the Compton scattered gamma rays due to the broad beam geometry setup used. Another striking feature is the fact that the various spectra, for a given absorber position, intersect one another at some point. This intersection point is also seen to depend on the absorber position, shifting towards the photopeak as the distance between the absorber and the detector increases. This is evident from Table 5-I, wherein the estimated positions (in keV) of the intersection point are given for the four absorber positions.

TABLE 5-I

	L = 0 cm	L = 5 cm	L = 10 cm	L = 15 cm
Estimated point of intersection (E in keV)	330 ± 20	405 ± 20	440 ± 20	445 ± 20
Maximum angle of scatteing (θ)	90°	67°	55°	56°
Compton energy (E_C in keV)	288	370	427	400

As mentioned earlier, in fig.5.1, θ is the maximum angle at which gamma rays scattered from the absorber can reach the detector. The energy of the Compton-scattered gamma ray is given by the expression

$$E_C = E_\gamma / [1 + \alpha (1 - \cos \theta)] \qquad \text{---------------- (5.1)}$$

where $\alpha = E_\gamma / m_o c^2$. In a narrow beam geometry, the number of in-elastically scattered gammas reaching the detector will be minimized. It is therefore expected that all parts of the

spectrum will get attenuated by the same factor exp(-μt) for a given absorber thickness, μ being the attenuation coefficient for the incident gamma rays. So when normalized spectra like those in figure 5.2 – 5.5 are plotted, they are expected to overlap one another everywhere. In broad beam geometry Compton-scattered gamma rays also get detected and contribute to the spectra in the energy region below the photopeak. The spectral counts per channel will therefore, increase as t increases. The lower energy part of the spectrum gets enhanced relative to the photopeak as t is increased, down to the minimum energy possible i.e, E_C corresponding to the maximum angle θ (Table 5-I). Below this energy, one expects overlapping of the normalized spectra. However, we actually see increasing suppression in the energy region below E_C as the absorber thickness increases. This behaviour can be explained as due to the presence of the backscatter peak at 188 keV (E_C for θ = 180) [See reference 3 and Chapter IX]. This peak corresponds to gammas of the lower energy indicated, falling on the absorber along with the gammas of 662 keV energy. The attenuation coefficient is larger for the backscattered energy and hence the observed behaviour below E_C. The changing value of E_C as the absorber position changes is seen to be nicely correlated to the change in the intersection point in the figures 5.2 - 5.5.

References

1. Evans R.D., "The Atomic Nucleus" (Tata McGraw Hill Publishing Co. – 1955) p. 728

2. Karunakaran Nair K., Unnikrishnan M.P. and Varier K.M., National symposium on Radiation Physics, NSRP – 13, Mangalore (1999) 547

3. Varier K.M.and Karunakaran Nair K., Radiat. Phys. Chem. Vol.51,No.4 – 6, (1998) 461

EFFECTIVE ATOMIC NUMBERS BY GAMMA ABSOPRPTION STUDIES

CHAPTER VI

EFFECTIVE ATOMIC NUMBERS BY GAMMA ABSOPRPTION STUDIES

6.1 Introduction

The concept of Z dependence of photon interaction has many applications in radiation studies and other fields involving radiation transport through materials. The effective atomic number has proved to be a convenient parameter for interpreting the gamma ray attenuation by a given medium.

Conventionally, the elemental cross section per atom is taken to be directly proportional to Z^m, where the index m depends on the particular interaction process being considered. A compound or a mixture may be considered as a single element with an effective atomic number Z_{eff} given by

$$Z_{eff} = [\, \Sigma_i\, f_i\, Z_i^{\; m-1}\,]^{\; 1/(m-1)} \qquad \text{------------(6.1)}$$

where Z_i is the atomic number and f_i is the fractional content by weight of the i_th element in the absorber combination, with $\Sigma_i\, f_i = 1$. It follows that the mass attenuation coefficient can be expressed as follows using the mixture rule [1] :

$$(\mu\,/\,\rho) = \Sigma_i\, f_i\, (\mu\,/\,\rho)_i \qquad \text{----------------(6.2)}$$

To characterize photon interactions, different effective atomic numbers have to be used for different individual processes over the extended energy range. The exponents

need not only vary with energy, but also become different at a given energy as the elemental composition changes. One of the important applications of the Z dependence of the photon cross section is the evaluation of the computerized tomography scans.

In view of the extensive use of the radio active sources in medicine, agriculture, industry etc., the study of photon – atom interaction (attenuation and absorption coefficients) in different materials has gained importance in recent years. Since these interactions involve various compounds with different compositions, the effective atomic numbers Z_{eff} for the total and partial gamma ray interactions in compounds are equally important. However the number of attempts to compile Z_{eff} are very limited. References [2 – 9] provide the work quoted in the literature to date on the effective atomic numbers.

We have carried out a few measurements at a gamma energy of 662 keV for various combinations of aluminium, copper, mercury and lead absorbers. The details of the experimental set up and the results are given in the following sections. A part of the present work has been presented at the Fourteenth National Symposium on Radiation Physics (NSRP 14) held at Amritsar in November 2001 [10].

6.2 Experimental Method

The 662 keV gamma rays for the measurements have been obtained from a 0.5 mCi ^{137}Cs source supplied by BARC, Mumbai. A well defined narrow beam geometry in a vertical set up was use for the attenuation measurements. The lead, aluminium and

copper absorbers were in the form of square sheets of dimensions 5 cm X 5cm and thickness of 0.1 mm, 1mm and 1 mm respectively. In the case of mercury, a 5 ml glass beaker was used for containing the liquid absorber. The absorber thickness in this case was varied by taking different volumes of the liquid in the beaker. The mercury level was measured by a precision traveling microscope. Measurements were made for various absorber thickness for the pure elemental absorbers and for various combinations of these. These various combinations were obtained by stacking the individual absorbers one over the other in the vertical narrow beam geometry, as shown in fig. 6.1.

For combination of mercury with the other absorbers, suitable numbers of absorber sheets were kept above the beaker containing the appropriate volume of mercury. It is assumed here that such combinations simulate a true mixture with a uniform composition. A 2" X 1 ¼" (Harshaw) NaI(Tl) detector mounted on a RCA 6810A PMT was used for detecting the gamma rays transmitted through the absorbers. The output of the pre amplifier is fed to a ORTEC 571 Amplifier and then to a CAMAC based data acquisition and analysis setup, consisting of a Kinetic CAMAC crate and controller, a 4k Quad ADC supplied by Electronics Division, BARC, Mumbai, and a PC via an interface card. The data acquisition and analysis was carried out using FREEDOM software [11] developed at the Nuclear Science Centre, New Delhi.

The attenuation coefficient in cm^2/gm have been calculated from the plot of logarithm of the transmitted intensities vs. the absorber thickness in gm/cm^2. An effective atomic mass number is evaluated for each absorber combination by the following expression :
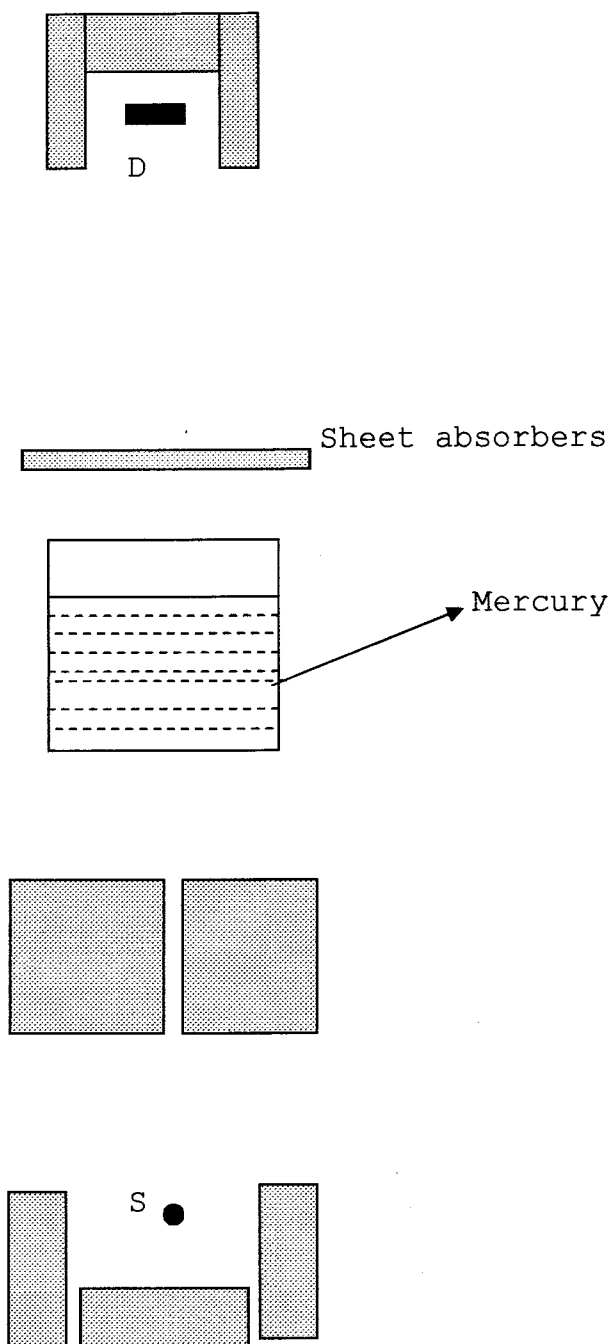
Fig. 6.1. Vertical narrow beam geometry set up

$$A_{eff} = \Sigma_i\, f_i\, A_i \qquad\qquad (2)$$

Where f_i is the fractional weight of the ith element with a mass number A_i .

The extracted attenuation coefficients in cm^2/gm were multiplied by A_{eff} to get the effective total interaction cross section in barns / atom. By a similar procedure, theoretical values were extracted using the XCOM package [12]. The effective atomic number of the absorber is calculated as per equation (1) above.

6.3 Results and Discussions

The experimental values for the total gamma interaction cross sections are plotted in figures 6.2 – 6.5 by means of the solid points vs. the effective atomic number for the incoherent scattering, coherent scattering, photoelectric absorption and for the total interaction respectively. Theoretical XCOM values for the mixtures are plotted as solid curves. Also plotted using the dashed curve are the XCOM results for elemental absorbers (i.e; for Z_{eff} = an integer, this is the approximation of a mixture where there is only one component in it, i.e; $f_i = 0$ except for i = this particular element). The good agreement between the experimental values and the XCOM results suggest the usefulness of the concept of effective atomic numbers for gamma ray interaction.
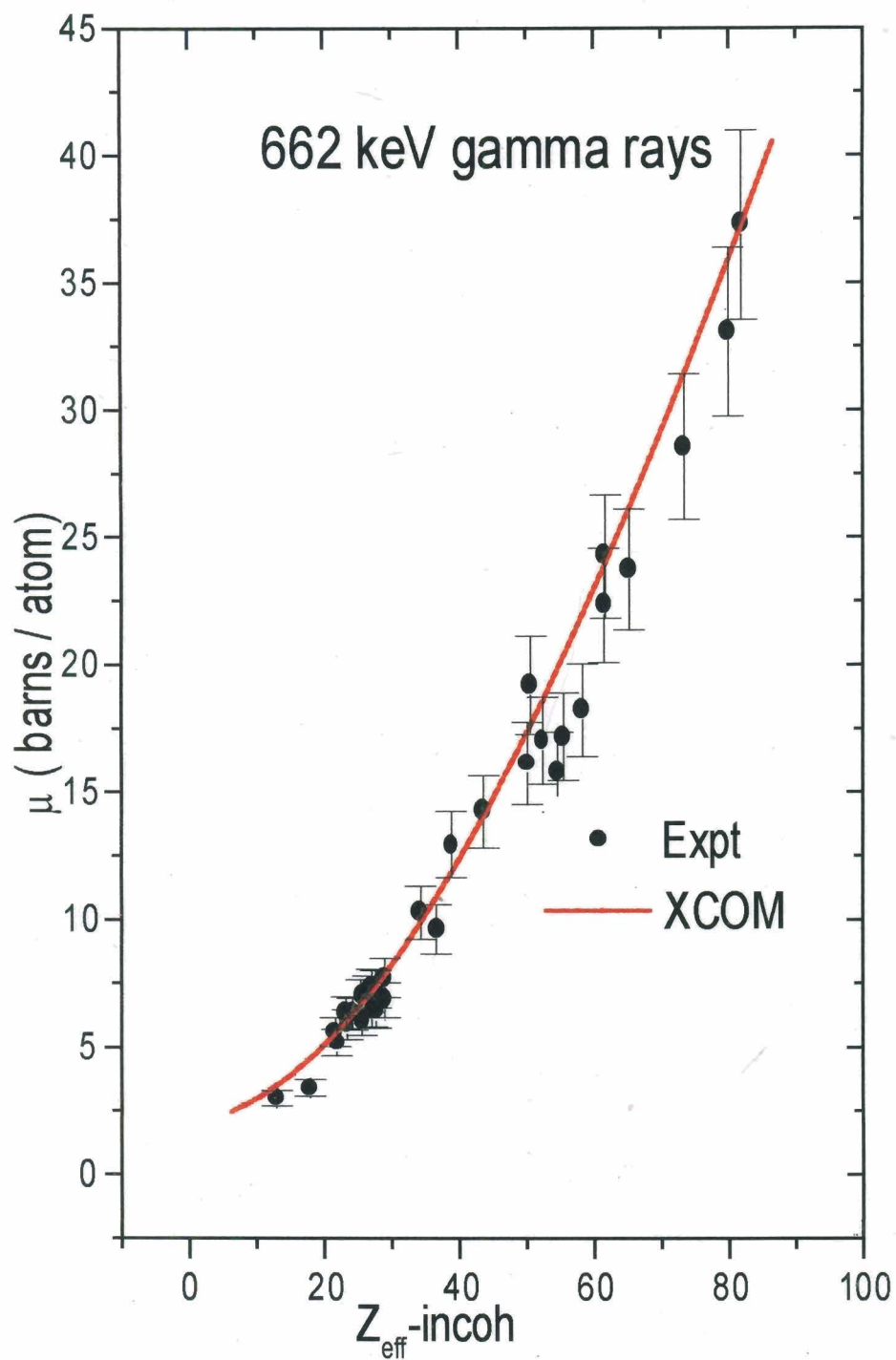
Fig 6.2. Variation of the total interaction cross section vs. effective atomic number for incoherent scattering
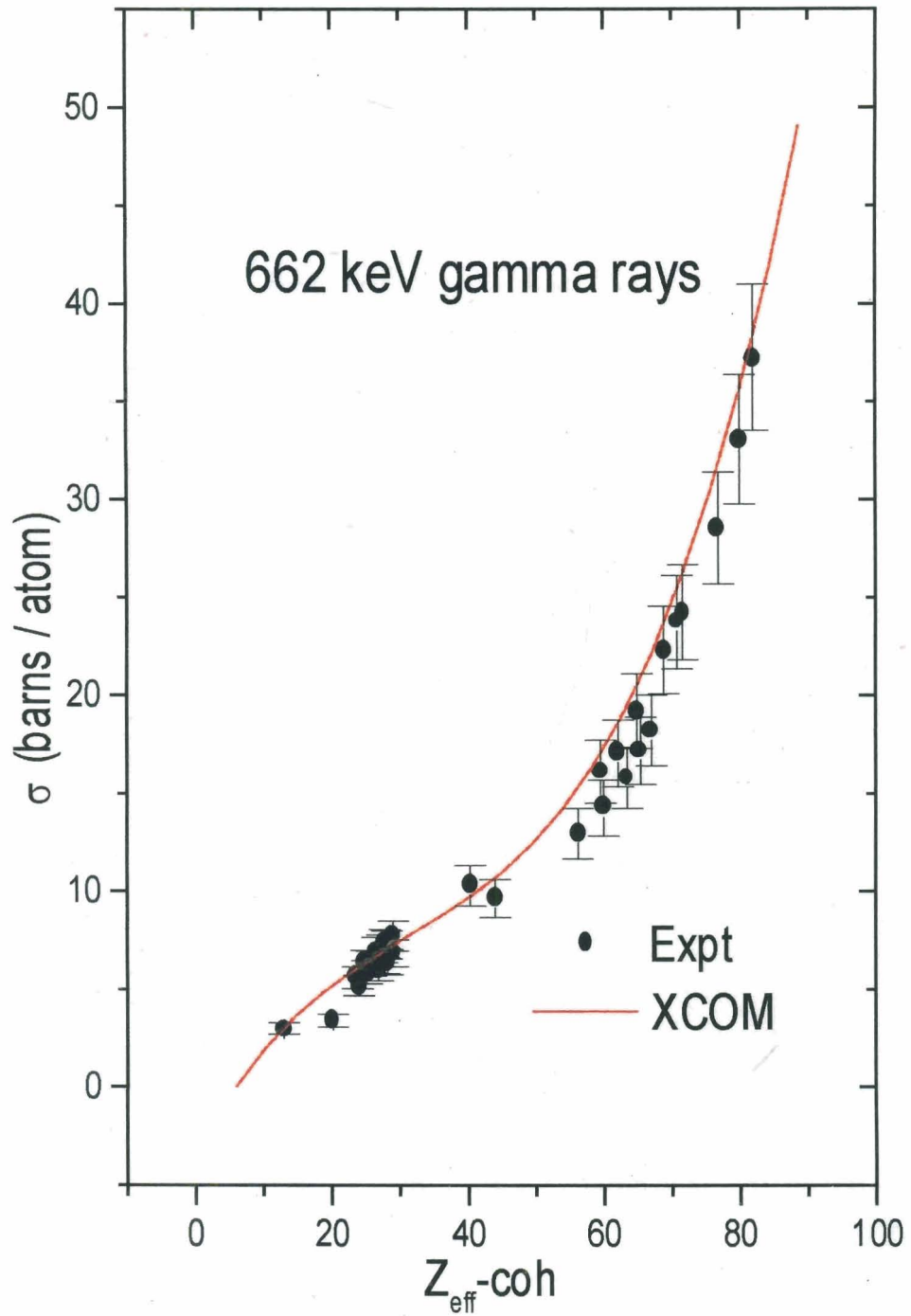
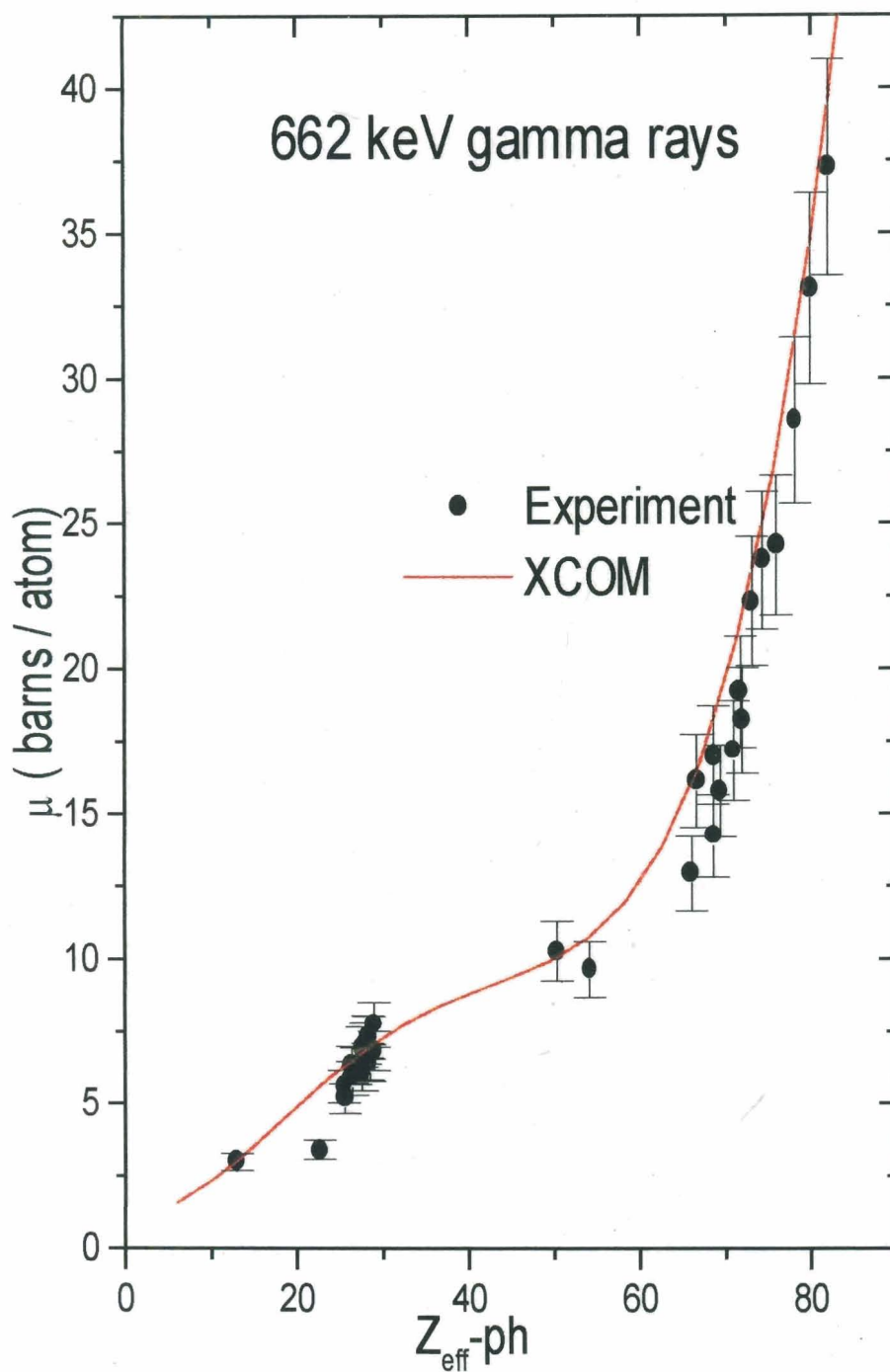Fig 6.3. Variation of total interaction cross section vs. effective atomic number for coherent scattering

Fig 6.4. Variation of the total interaction cross section vs. effective atomic number for photoelectric absorption
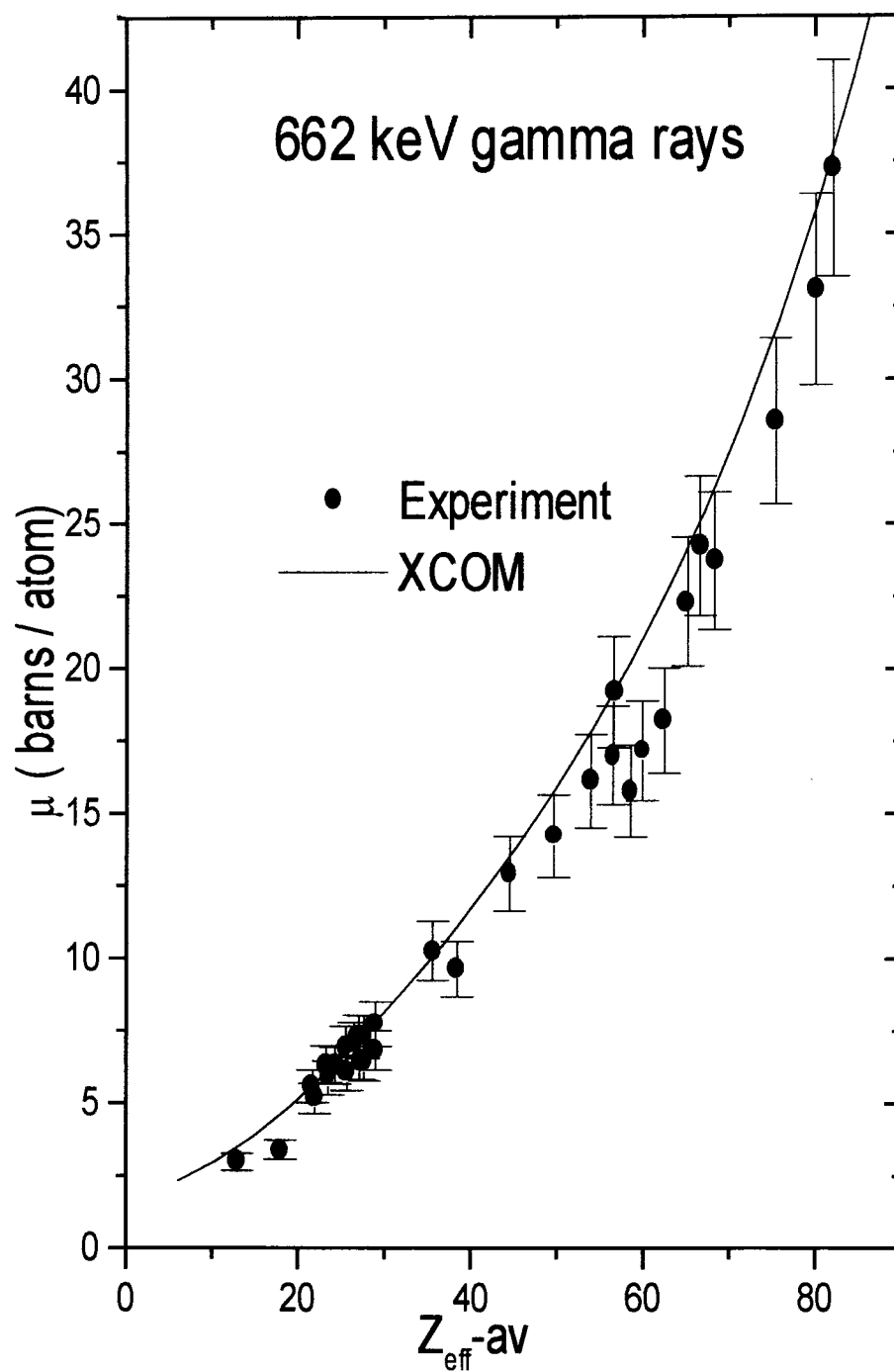
Fig 6.5.Variation of the total interaction cross section vs. effective atomic number for total interaction

REFERENCES

1. Evans R.D., "The Atomic Nucleus", and J.H.Hubbel, Report NSRDS (1969) 29

2. Hiremath S.S. and Chikkur G.C., Ind. J. Pure & App. Physics, 31 (1993)855

3. Krishna Reddy D.V., Suresh Babu K. and Chandralingam S., Can. J. Phys. 63(1985)1421

4. Parthasaradhi K., Ind. J. Pure & App. Phys., 6(1968) 609

5. Perumallu A., Nageswara Rao A.S.and Krishna Rao G., Can. J. Phys, 62(1984)464

6. Chandralingam S., Suresh Babu K. and Krishna Reddy D.V., Ind. J. Phys. (1984)285

7. Bhandal G.S.and Singh K.S., App. Rad. & Isotop. 44(1993)1231

8. Kumar T.K. and Reddy K.V., Rad. Phys. And Chem., 50(1997)545

9. Shivaramu, R. Vijayakumar, L. Rajasekharan and N. Ramamurthy, Proceedings of ISRP-14, Amritsar, November 2001 (p. 153)

10. Karunakaran Nair K., Abdul Gafoor A.K., Jeeja V.S., Ramachandran N. and Varier K.M., Proceedings of ISRP-14, Amritsar, November 2001 (p. 137)

11. Ajithkumar B.P.and.Subramanyam E.T, "FREEDOM" (1995)

12. Berger M.J. and Hubbel J.H., NIST Standard Reference Data Base (1990)

GAMMA ATTENUATION STUDIES IN LIQUIDS

CHAPTER VII

GAMMA ATTENUATION STUDIES IN LIQUIDS

7.1 Introduction

There are some circumstances where we have to deal with absorbers whose thickness and / or composition varies with time. Examples are i : flow of water in and out of a water tank, ii : evaporation of a volatile liquid kept in a vessel, iii : rotating absorber with non uniform composition of thickness etc. The gamma ray attenuation / transmission in such cases can be applied easily in such cases for studying the time variations involved.

In most multi channel analyzers there is a particular mode of operation called Multi channel scaling (MCS). This mode is best suited for studies where the number of output pulses from a radiation detector is time dependent. The MCA, operated in the MCS mode will provide a plot of total gamma counts vs time. A classic example is the application in Mossbauer studies.

We have utilized the above facility of the MCA for the present studies. In this chapter the studies on the first two examples given above viz;

I flow of water in and out of a water tank

II evaporation of a volatile liquid kept in a vessel

The application to rotating non uniform absorbers is explained later in chapter 8.

7.2 Gamma attenuation studies on evaporation of a volatile liquid

At any given temperature, a liquid contained in a vessel will be subjected to the process of evaporation from the top surface. If the ambient temperature is very much above the boiling point, as in the case of liquid nitrogen, the liquid also will boil at the surface. There will be a gradual variation of the vapour density as we go up from the liquid surface. When a gamma attenuation measurement is made in a fixed narrow beam good geometry set up, the transmission of the gamma rays will change with time as the evaporation proceeds, both in the vertical and horizontal directions. We have investigated the consequent variation of the attenuation coefficient using 662 keV gamma rays. The following sections give the details of the experimental setup and the main results. A part of the work had been presented at the Fourteenth National Symposium on Radiation Physics held at Amritsar in November 2001 [1].

7.2.1 Experimental details

The present measurements have been carried out using 662 keV gamma rays from a 0.5 mCi ^{137}Cs source, procured from BARC, Mumbai. Liquid nitrogen was taken in a rectangular trough made of thermo cool material. The incident gamma rays were well collimated by means of a channel of 3mm X 3mm rectangular cross section, transmitted

through the absorbing liquid and detected by a 2" X 1 1/4" NaI(Tl) detector, coupled to a RCA 6810A Photo multiplier tube, pre amplifier and an ORTEC 571 amplifier. The amplifier output pulses were then fed to a CAMAC based data acquisition and analysis system, consisting of a Kinetic CAMA crate, crate controller, a 4k Quad ADC, supplied by the Electronics Division, BARC and connected to a Personal Computer through a suitable interface card. A Linux based package, FREEDOM, developed at the Nuclear Science Center, New Delhi [2] was used for the data collection and analysis.

7.2.2 Results and Discussions

Figures 7.1(a) and 7.1(b) give the geometry of the set up in the horizontal and vertical geometries. In both geometries, the initial height of the liquid in the container was 5.8 cms. In the horizontal geometry, the top surface was at a height of 3.4 cms above the level of the gamma ray beam. As the liquid evaporates, the liquid level comes down, crosses the gamma beam and then falls further down. The observed variation in the transmission of the gamma rays through the liquid nitrogen (and the vapor above the top surface in the vertical geometry) as a function of time is plotted in figures 7.2(a) and 7.2(b). The results are as expected.

In the vertical geometry the path length of the gamma rays through the liquid decreases as the liquid evaporates, whereas, in the horizontal geometry, the path length remains a constant. Transmission is a constant, equal to that through the entire length of the liquid nitrogen, until the level of the top surface of the liquid is just above the
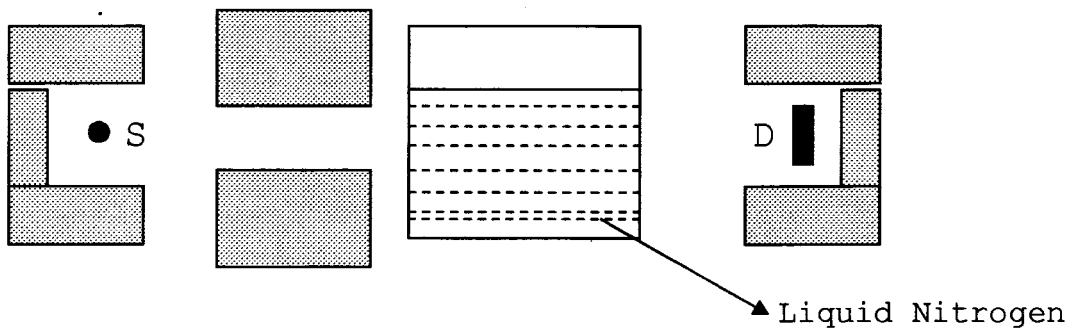
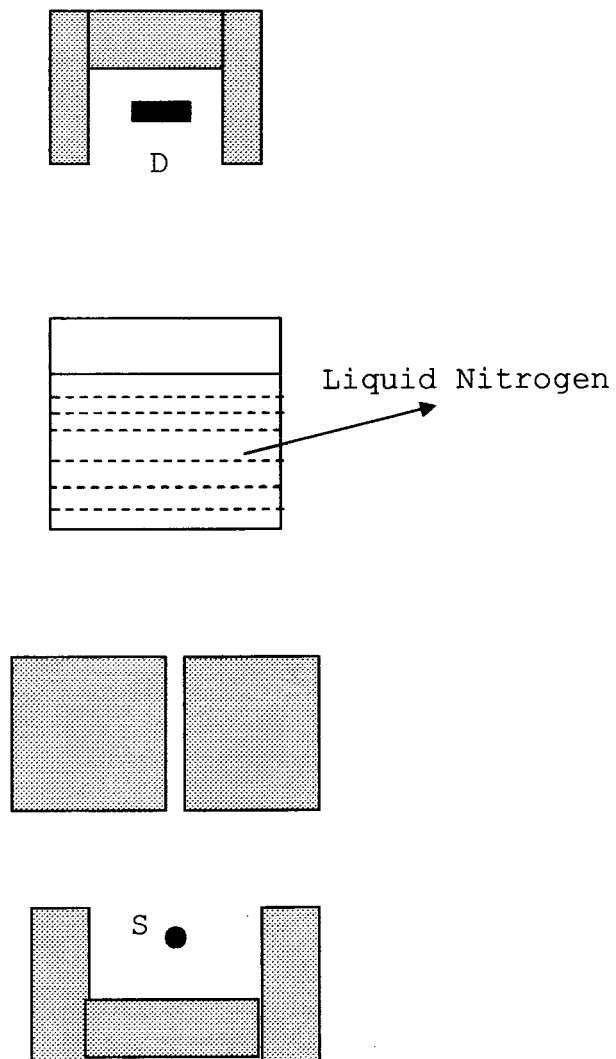Fig. 7.1a. Narrow beam geometry set up for the horizontal geometry

Fig. 7.1b. Narrow beam geometry set up for the vertical geometry

horizontal level of the gamma ray beam through the collimating channel. As the level crosses the gamma beam, transmission decreases relatively fast and drops again to a constant value, equal to that through air. In the transition region, transmission passes through intermediate values which will involve the attenuation through the nitrogen vapours of varying densities. The calculated value of the attenuation coefficient μ/ρ in the horizontal geometry is (0.075 ± 0.008) cm^2/gm. This agrees well with the XCOM [3] value of 0.07722 cm^2/gm.

The rate of evaporation of the liquid level was measured by measuring the liquid level as a function of time. The result is also plotted in figures 7.2(a) and 7.2(b) by the solid straight lines. The instant at which the level of the liquid is at the horizontal level of the gamma beam in the horizontal geometry is 52.8 minutes. This correlates well with the time at which the transition in the transmission value occurs (i.e; the time at which the level is that of the horizontal gamma ray beam, 2.4 cms). This time is marked by the point P in the figures.

A typical MCS spectrum obtained in the present work for the horizontal geometry is shown in figures 7.3.
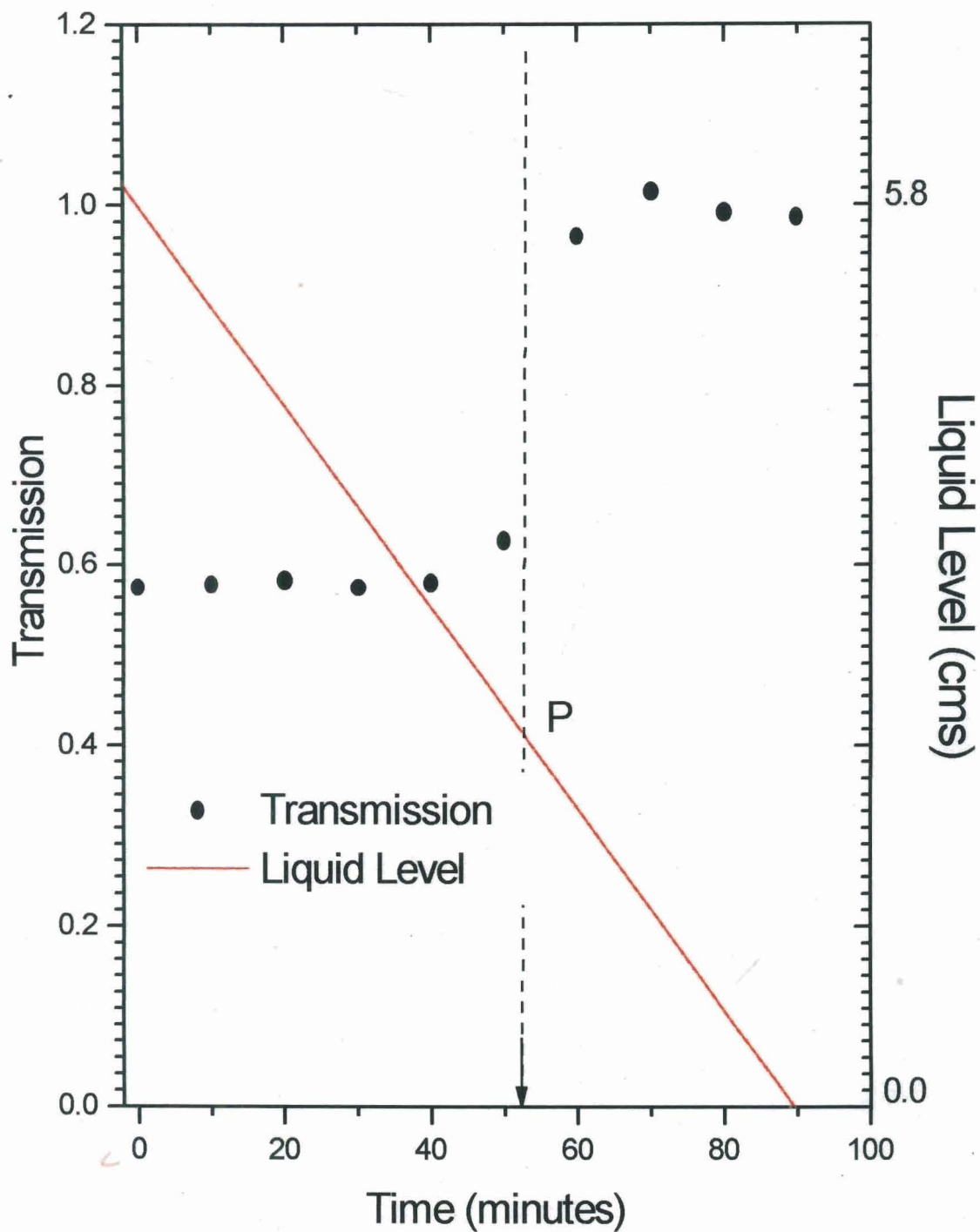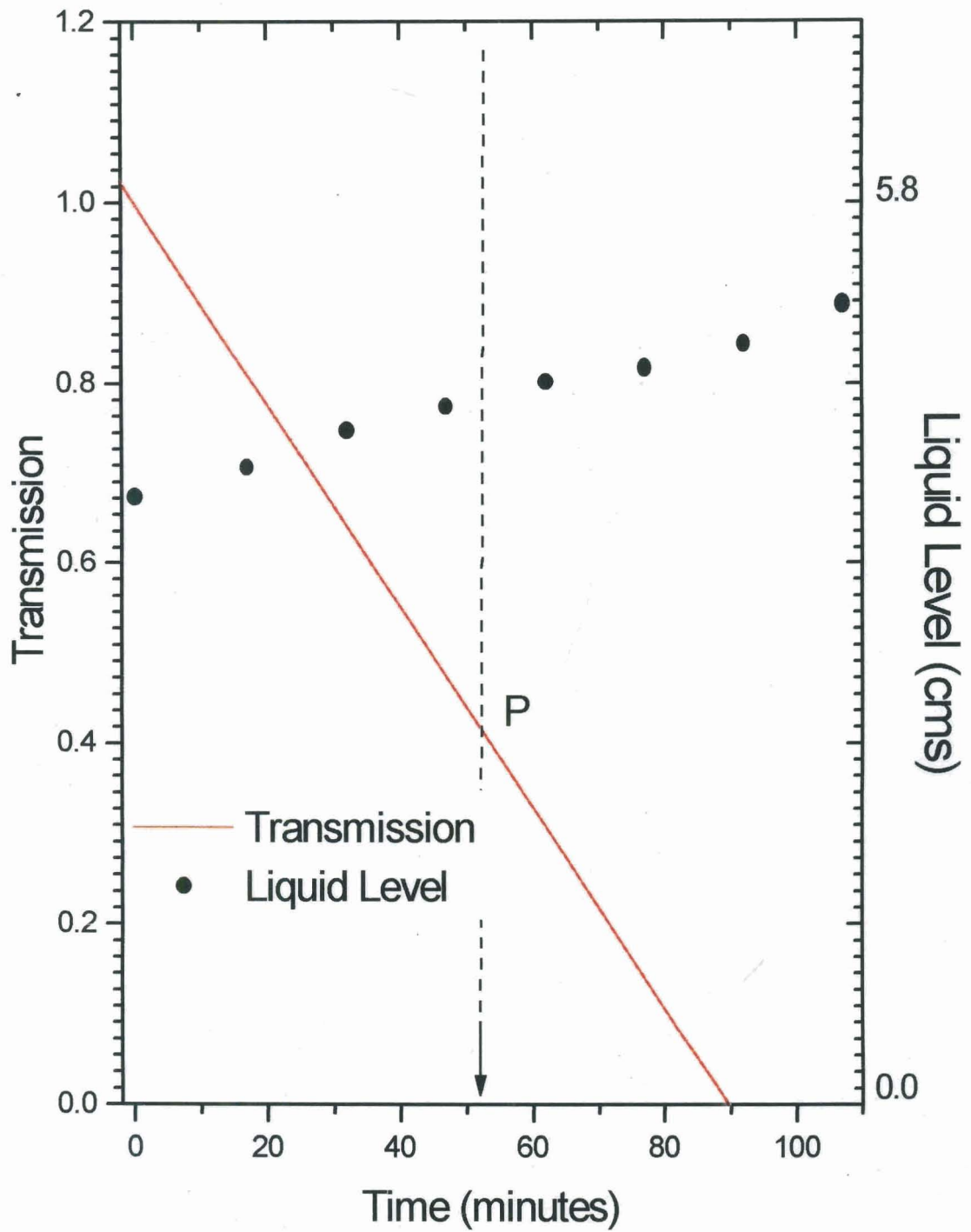
Fig 7.2(a) Results for the horizontal geometry

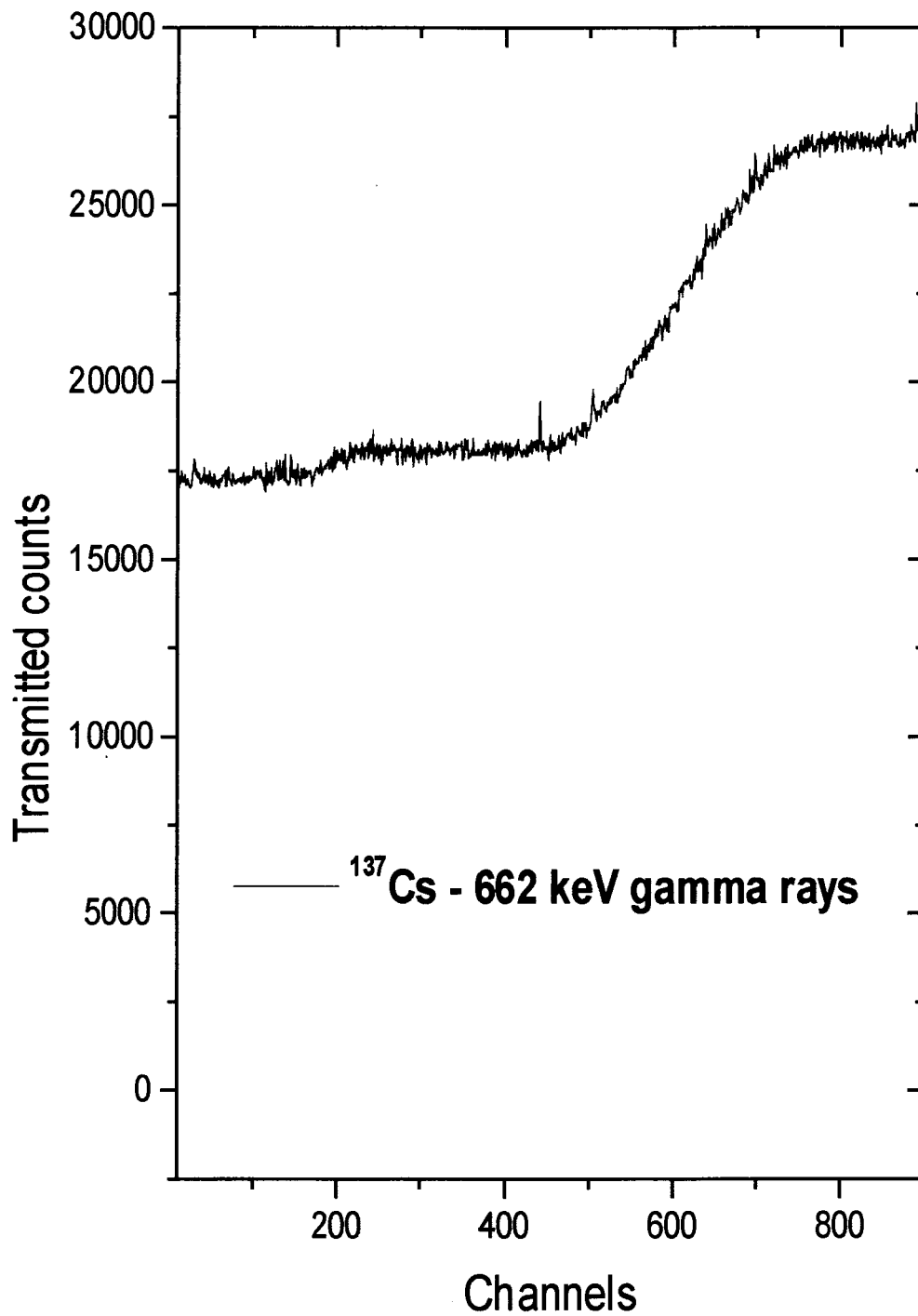Fig 7.2(b) Results for the vertical geometry

Fig. 7.3 - Transmitted counts vs time taken with MCA in MCS mode

7.3 Gamma attenuation study on flow of water in and out of a tank

7.3.1 Absorbers

The absorber in this experiment is water taken in a beaker. An arrangement is made for letting the water in and out of the beaker at variable rates. The variable rates were obtained by adjusting the height of the storage tank / beaker.

7.3.2 Source, Detector and Electronics

The source ^{137}Cs, is the same as the one used in the investigations described in section 7.2.1 above. Essentially the same detector and electronics were also used. The multi channel analyzer, however, was a Nucleonix 4K MCA, operated in the MCS mode. The dwell time per channel was suitably selected, such that the relevant time variations are seen within the total number of channels selected (normally 4k).

7.3.3 Results and Discussions

Figures 7.4 – 7.7 show typical MCS spectra for the experiment where a beaker, filled with water, is allowed to drain completely, by letting out the water at controlled rates. A calibration curve can be plotted, wherein the measured transmissions are plotted as a function of height of liquid in the beaker. Combining the MCS spectrum and the calibration, it is possible to study the flow rate of the liquid as a function of time.

7.4 Conclusions

The results are encouraging. A possibility of using the gamma ray attenuation method for liquid nitrogen level monitoring as well as for monitoring of levels of other liquids is suggested by the present results.
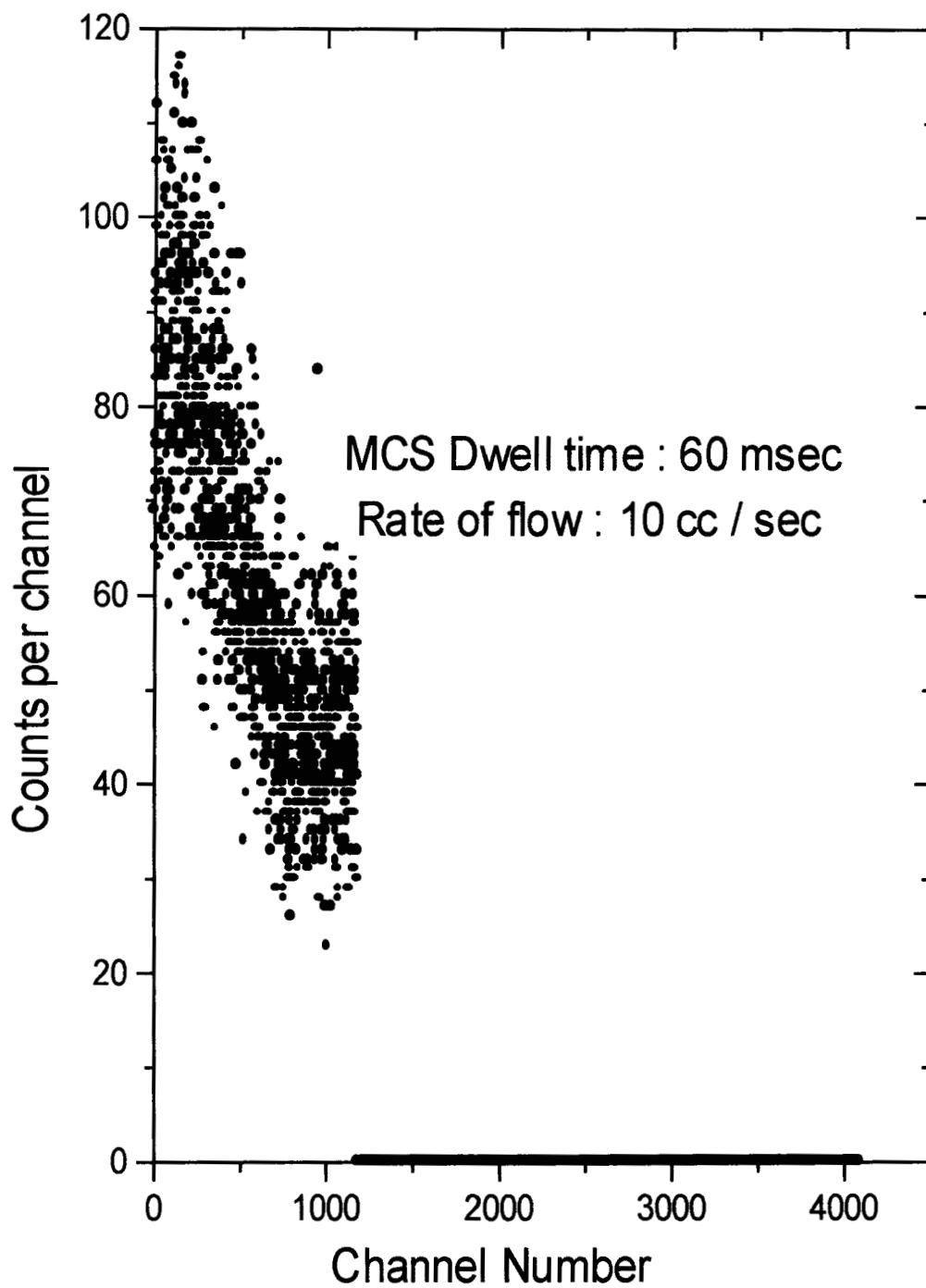
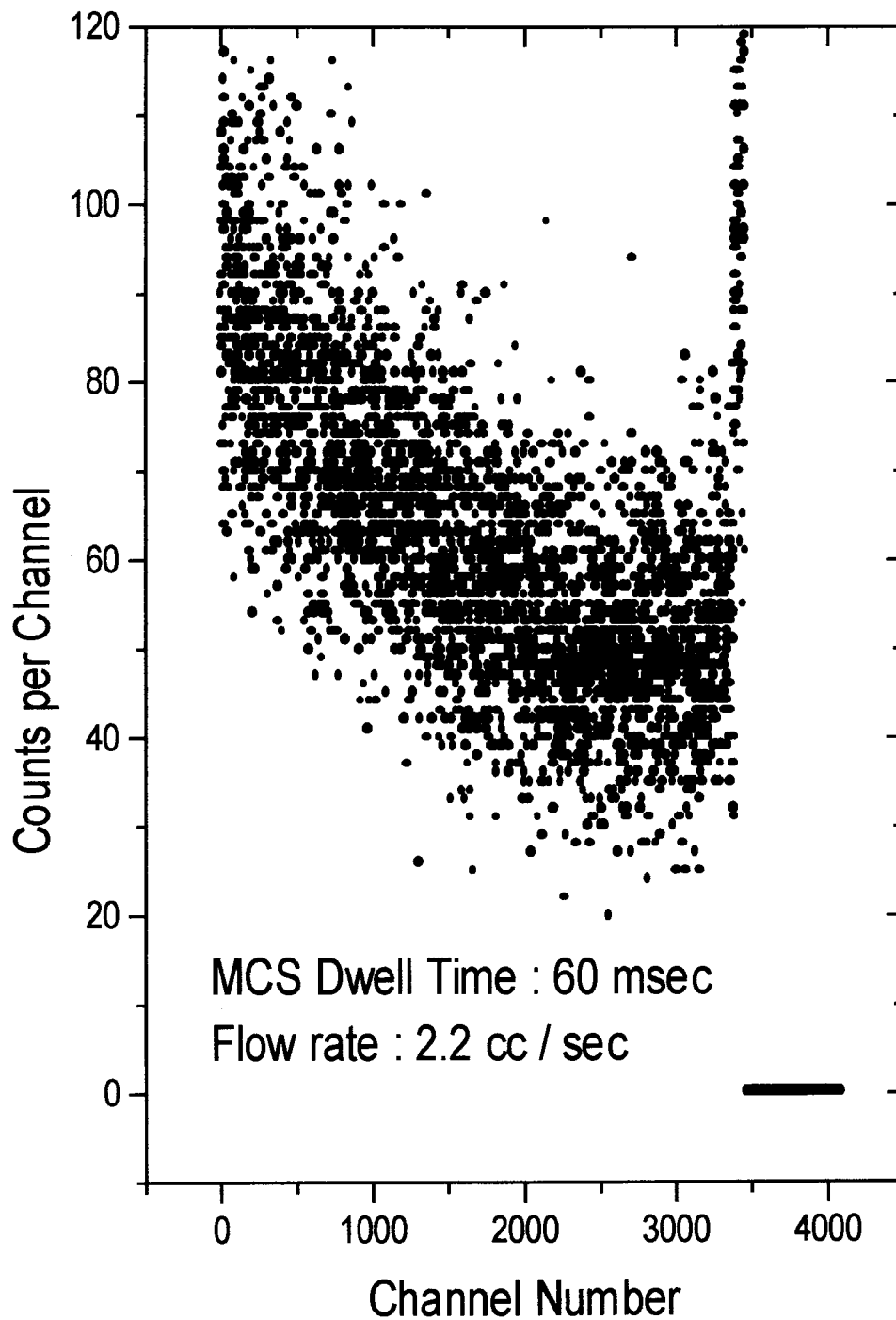Fig 7.4 - MCS spectrum of the transmitted gamma rays for water flowing out of a beaker at constant rate

Fig 7.5 - MCS spectrum of transmitted gamma rays
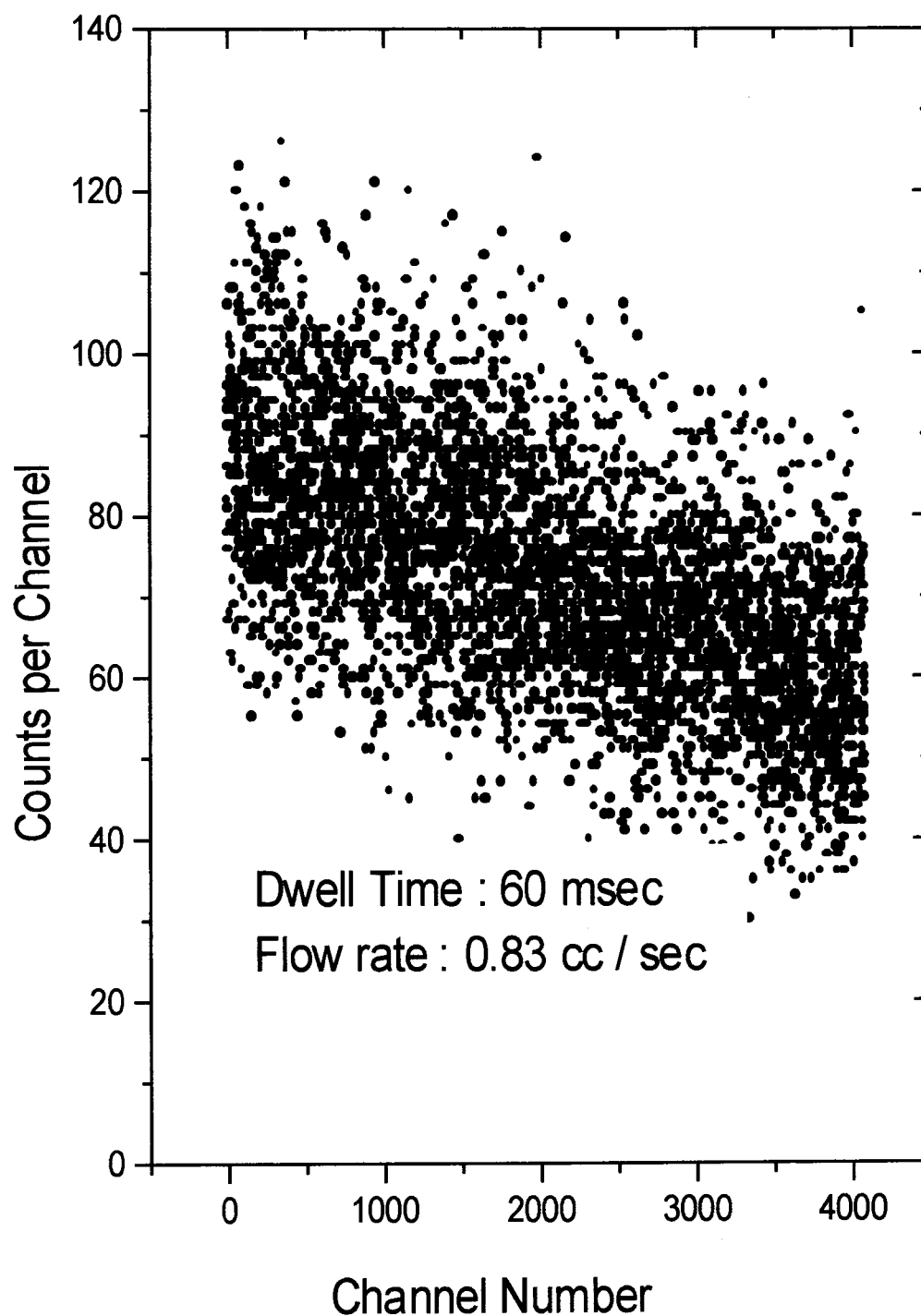through water flowing out of a beaker at constant rate

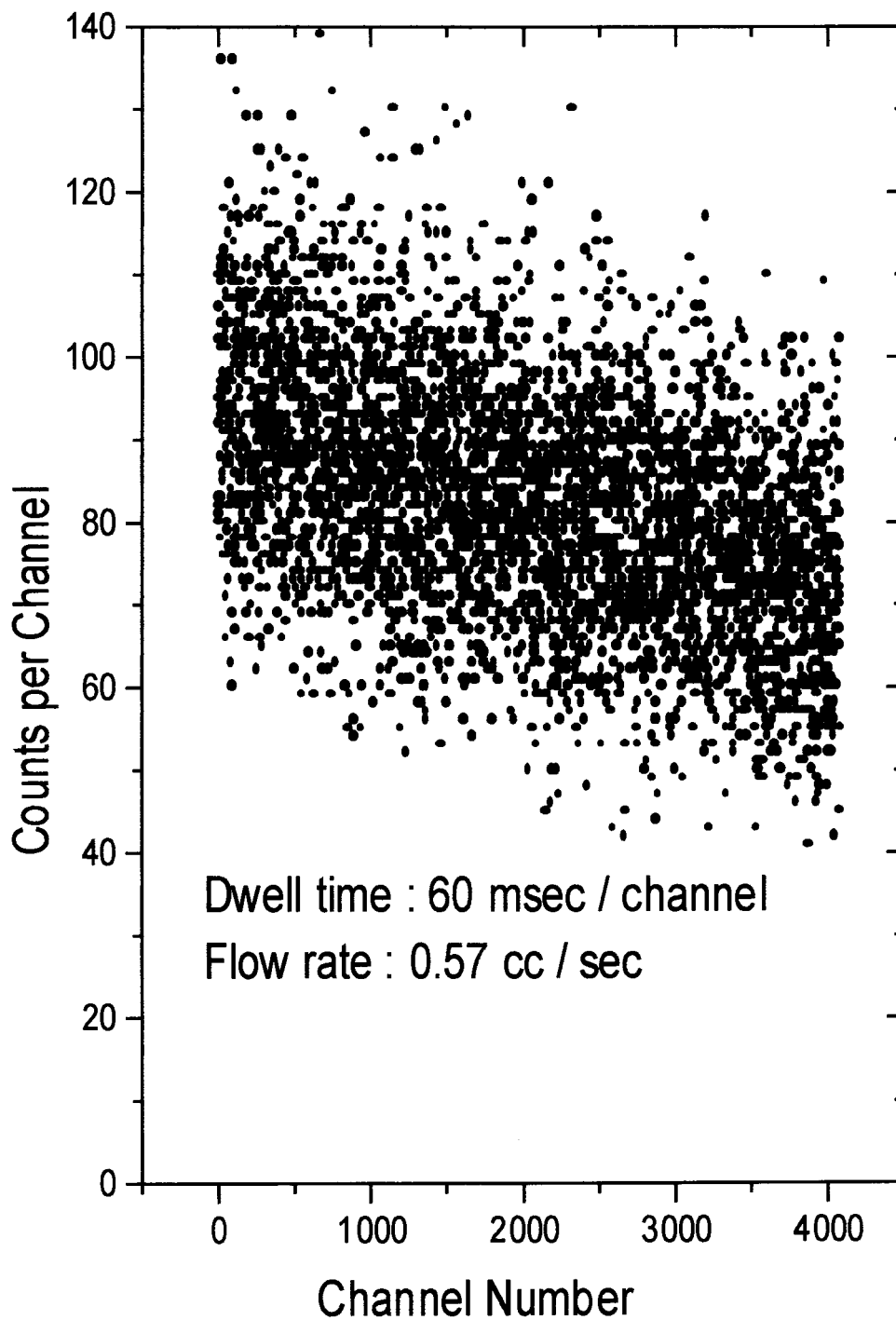Fig 7.6 - MCS spectrum of gamma rays transmitted through water flowing out of a beaker at constant rate

Fig 7.7 - MCS spectrum of gamma rays transmitted through water flowing out of a beaker at constant rate

References

1. Karunakaran Nair K., Ramachandran N. and. Varier K.M, Proceedings of the Fourteenth National Symposium on Radiation Physics, Amritsar (2001) 145

2. Ajithkumar B.P. and Subramanyam E.T., "FREEDOM" (1995)

3. Berger M.J. & Hubbel J.H., NIST Standard Reference Database 1990

EXPERIMENTAL STUDIES ON ROTATING ABSORBERS

Chapter VIII

EXPERIMENTAL STUDIES ON ROTATING ABSORBERS

8.1 Introduction

In many applications of gamma radiations the absorbers are in the form of mixtures of elements/ compounds. The effective transmission through such absorber is governed by the mixture rule [1] . As already explained in earlier chapters , the effective mass attenuation coefficient of the mixture is governed by the expression

$$(\mu/\rho)_m = \sum_i w_i \, (\mu/\rho)_i \qquad\qquad \ldots\ldots\ldots\ldots\ldots (8.1)$$

where w_i are the weight fractions of the ith element whose mass attenuation coefficient is $(\mu/\rho)_i$. Practically we can view the action of a mixture on the gamma ray photon, as it traverses the material, in the following way. Consider one gamma ray photon in the incident beam. It is removed from the beam in a single interaction. This will take place with a particular constituent element of the mixture. The next incoming photon may interact with another constituent element and so on. The effect would be same if , by the time the second photon arrives at the absorber position, the first elemental absorber is replaced by the second absorber and so on. In practice, this can be achieved by using an absorber in the form of a disc, which is composed of different sectors, each sector being composed of a different absorber. This disc is rotated about an axis passing through its center such that each elemental absorber comes in position between the source and

detector, one after the other. In this way, the mixture absorber can be simulated. Fig. 8.1 gives the schematic diagram of the setup.

Consider the simple case of a thin disc of a single element, with uniform thickness t_0. In this case, absorber rotation does not affect the gamma transmission in any way. The same thickness of the same elemental absorber is presented to the incoming photons always. We get

$$I = \tau\, i_0\, \exp(-\mu_0\, t_0) \qquad\qquad \text{------------------- (8.2)}$$

for one period of rotation τ of the absorber. Here i_0 is the incident number of photons per second.

Now consider a narrow strip of absorber of a different element of length l of thickness t fixed on to this disc at a distance of r cms from the center, such that this strip will occupy the absorber position once in a rotation. The angle subtended by the absorber at the center of the disc is $\theta = l / r$. So, in one rotation, this new elemental absorber comes in the path of the photon for a time equal to $(\theta / 2\pi)\, \tau$.

Now, if the observations are carried out over a large number of periods, say, n, the transmitted intensity will be

$$I = n\, \tau\, i_0\, \exp(-\mu_0\, t_0)\, \{\, (1 - \theta / 2\pi) + (\theta / 2\pi)\exp(-\mu\, t)\, \} \quad \text{----- (8.3)}$$
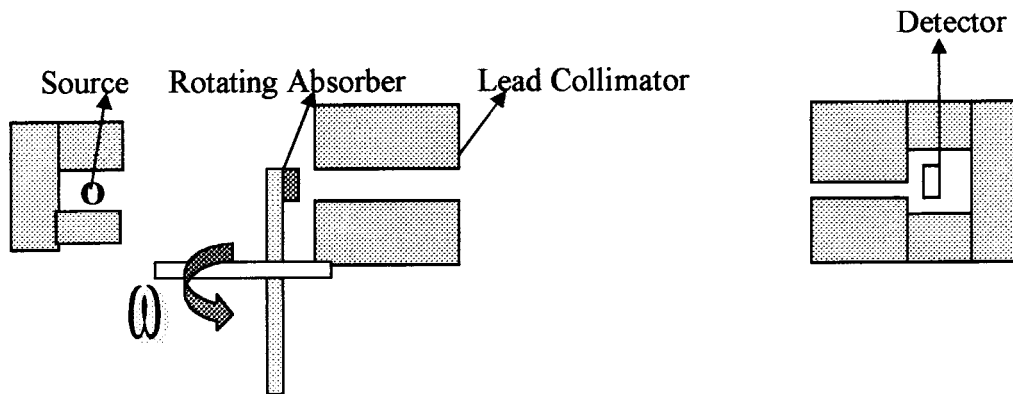
Fig. 8.1 Schematic diagram of the experimental setup for narrow beam geometry gamma attenuation measurements using rotating targets

This can be written as

$$I = \tau \, i_o \, \exp(-\mu_{eff} \, t_{eff}) \quad \text{---(8.4)}$$

where

$$\exp(-\mu_{eff} \, t_{eff}) = (1 - \theta/2\pi) + (\theta/2\pi) \exp(-\mu t) \quad \text{------------------(8.5)}$$

Thus the rotating target would simulate a mixture absorber. We can define an effective atomic number Z_{eff}.

$$Z_{eff} = (\theta/2\pi) Z \quad \text{---(8.6)}$$

where Z is the atomic number of the elemental absorber used.

In the general case, we may have 'n' elemental absorbers, Then

$$Z_{eff} = (1/2\pi) \Sigma \, \theta_i Z_i \quad \text{---------------------------------------(8.7)}$$

8.2 Experimental Set up :

A circular disc of diameter 20 cm is fabricated using Hylum sheet. Provision is made to fix absorbers at four positions on the disc. The arrangement to place absorbers are such that two positions are at opposite ends of the diameter. Suitable arrangements are made to fix the absorbers tightly on the disc. The disc is mounted on the shaft of a 1/8 hp ac motor such that the plane of the absorber is always perpendicular to the diameter of the gamma ray. A collimated beam of gamma ray is obtained from a ^{137}Cs source. The beam of gamma rays passes perpendicular to the plane of the disc. Hence it also passes through perpendicular to the absorber if the absorber is placed on the rotating disc. The speed of the motor is controlled by a UJT controlled SCR circuit . The

control circuit is fabricated such that the speed of the motor is constant and it is monitored using a opto-electronic arrangement. The absorbers are taken in the form of sheets of thickness 1mm and it is fastened on the disc. A NaI(Tl) detector with suitable electronic arrangement is used to detect the transmitted radiations. The output of the pre amplifier is fed to the CAMAC arrangement, which stores the spectrum and display it on the monitor using the FREEDOM software. The transmitted intensity (evaluated in terms of photo peak area in the transmitted gamma spectrum) is studied as a function of speed of rotation of the absorber and also as a function of the Z_{eff} as defined in equation 8.7. We have used copper and aluminium sheet absorbers of dimension 5 cm x 5 cm x1 cm.

Also, in order to see what is happening in each period of rotation , the transmitted total count have also been recorded with multi channel analyzer in MCS mode.

8.3 Results and Discussions

Fig 8.2 shows a typical MCS spectrum of the transmitted total gamma counts. The expected wavy nature of the MCS spectrum is worth noting. The crests correspond to the time periods when the hylum disc alone is in the gamma beam path and the troughs represent the time periods when the strip absorber also comes in the path. It is found that the transmission factor, evaluated from the MCS spectrum, by taking the ratios of the counts in the trough region and the crest region, agrees with the value evaluated from the pulse height spectra.
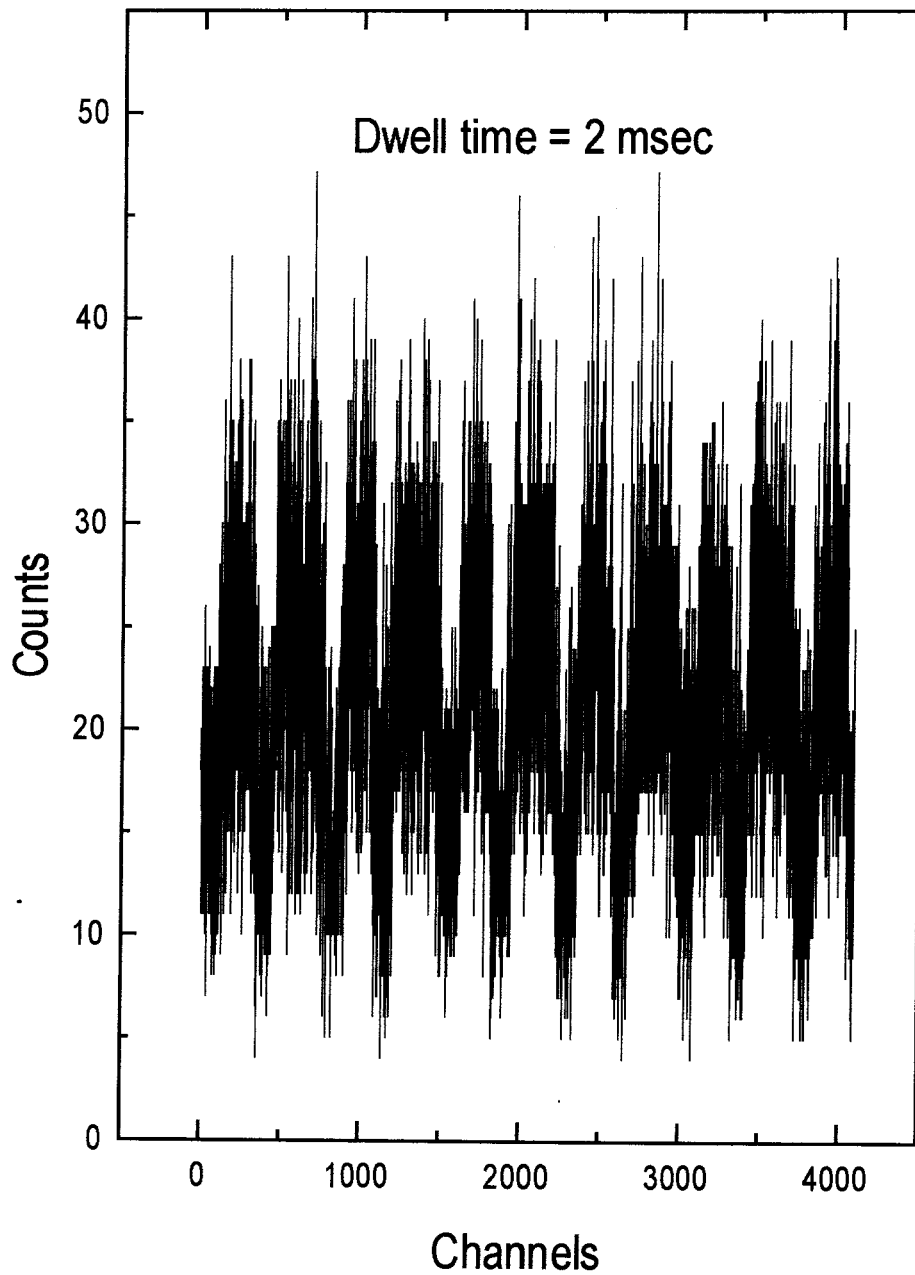
Fig 8.2 - MCS spectrum of gamma rays transmitted through rotating absorber

Table 8.1 gives the effective atomic number Z_{eff} and the corresponding atomic cross sections (derived from μ_{eff}) for the different absorber combinations investigated. For comparison, the values of μ_{eff} determined earlier (see chapter VI) for the respective Z_{eff} values as given in the last column of the table. The agreement between the two sets of values is quite satisfactory. Fig 8.3 plots the results in graphical form.

Table 8.1 – Effective atomic numbers and attenuation coefficients using rotating targets

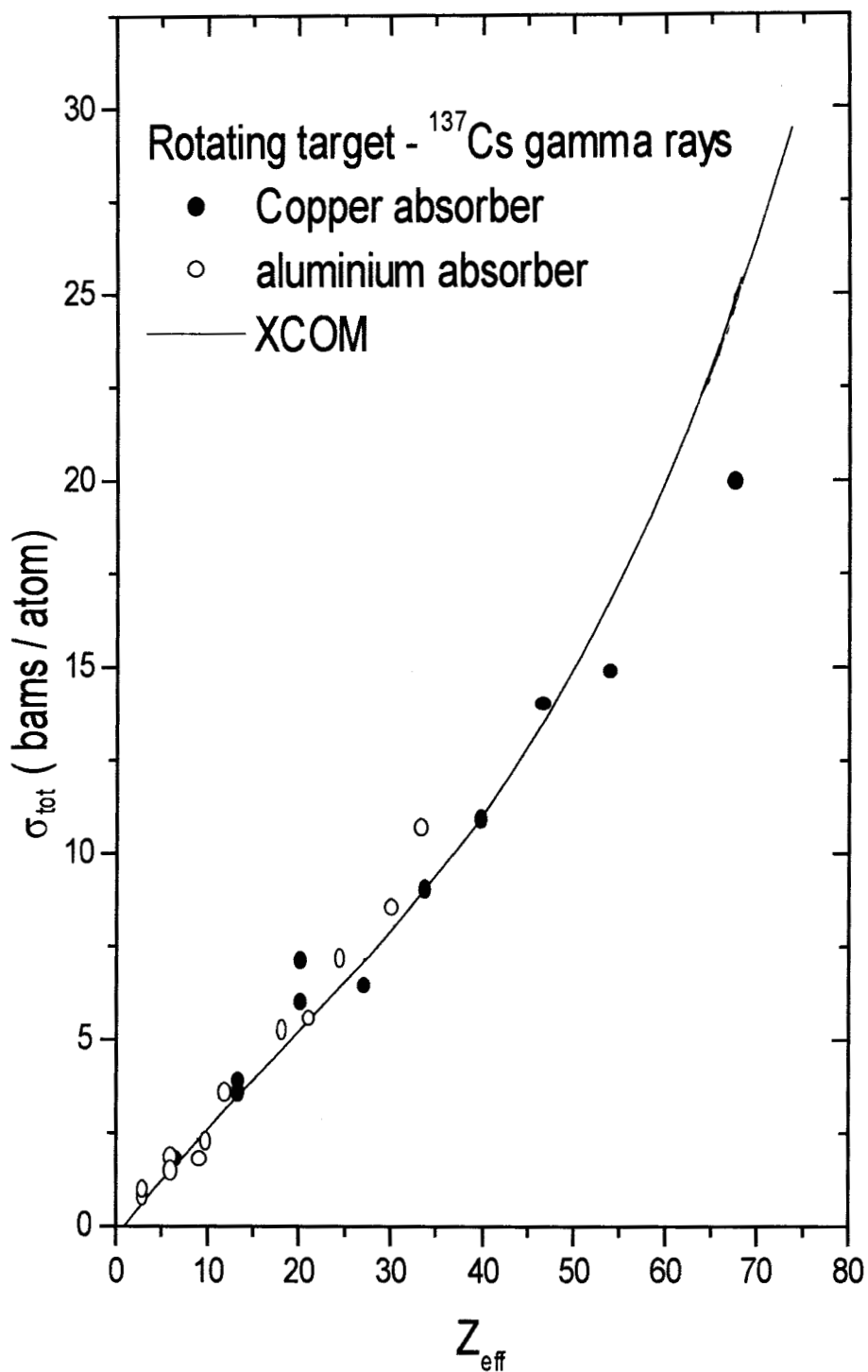| Sr. No	Atomic cross sections in b / atom Using rotating copper absorbers			Atomic cross sections in b / atom Using rotating aluminium absorbers		
	Z_{eff}	Present experiment	XCOM values	Z_{eff}	Present experiment	XCOM values
1.	6.67	1.8	1.74	3.03	0.79	0.77
2.	13.34	3.58	3.43	6.07	1.49	1.57
3.	20.31	7.10	5.27	9.91	2.30	2.56
4.	27.08	6.42	7.12	12.13	3.6	3.1
5.	33.85	9.01	9.10	18.20	5.29	4.71
6.	40.02	10.95	11.09	21.23	5.53	5.52
7.	46.69	13.98	13.56	24.64	7.19	6.44
8.	54.16	14.85	16.82	30.3	8.52	7.98
9.	67.7	19.97	24.87	33.37	10.67	8.97

Fig 8.3 - Photon cross sections vs. Effective
Atomic numbers using rotating targets

REFERENCES

1. R.D. Evans, "Atomic Nucleus", Tata McGraw Hill (1955) 713

EFFECT OF SOURCE BACKING ON THE BACKSCATTER PEAK IN GAMMA RAY SPECTRA

CHAPTER IX

EFFECT OF SOURCE BACKING ON THE BACKSCATTER PEAK

IN GAMMA RAY SPECTRA

9.1 Introduction

A typical pulse height spectrum of mono energetic gamma rays has two main characteristic structures, namely, the full energy or photo peak and the Compton distribution. The photo peak is due to complete energy absorption inside the detector by one of the absorption processes like photo electric effect , pair production etc. The Compton distribution is characterized by a continuous distribution of pulse heights starting from zero up to the so called Compton edge and corresponds to Compton scattering events inside the detector medium in which the scattered gamma ray photon escapes from the detector. In addition to these two prominent structures, another common feature of the gamma ray spectrum is the back scattered peak, arising out of the detection of gamma rays scattered at near backward angles from the surrounding materials. These could be shielding materials, the photo multiplier, source backing etc.

It can be seen from the expression for the energy of the scattered photons that beyond a scattering angle of about 120° or so, the scattered gamma ray energy is more or less insensitive to the scattering angle and is approximately equal to its value for $\theta = 180^\circ$, given by :

$$E_b \quad = \quad E\gamma \quad / (1 + 2\alpha) \qquad (9.1)$$

Here, E_γ is the incident gamma energy and α is the ratio of the gamma energy to the electron rest mass. Hence a mono energetic gamma ray source will give rise to many scattered gamma rays with energies near to this minimum value. Consequently, a broad peak appears in the spectrum. This is the so called back scattered peak [1].

The back scattered peak energy approaches the asymptotic value of 256 keV as the gamma energy increases. Thus the back scattered gamma ray peak is a source of interference in the energy region around and below 256 keV. It is therefore necessary to know the extent of the contribution of the back scattered peak in practical gamma ray spectra.

Back scattering from shielding materials can be minimized by increasing the dimensions of the shielding cavity relative to the crystal dimensions [2]. Also, a lining of low Z material can be incorporated on the inner walls of the shielding.

The source invariably has a backing and this will necessarily give rise to a back scattered peak. It will be interesting to study the effect of source backing on the back scattered peak. We have carried out such studies using ^{137}Cs and ^{60}Co sources using a Sodium iodide detector and a ^{57}Co source using HPGe detector.

9.2 Experimental details

A 1 ¾" NaI(Tl) detector was used for the measurements using the two higher energy gamma sources and an ORTEC HPGE detector has been used for measurements

involving the lower energy source. The radioactive sources with activities around 1 μCi

have been procured from BARC, Mumbai. The sources were already on backings. Extra

copper and lead backings were used for the measurements. These backings were mounted

behind the source. The thickness of the backings were varied from μt = 0 to about 2. The

spectra were collected and analyzed using a Nucleonix PC based Multi channel analyzer.

Data have been taken for two values of the source to detector distance, namely, 5 cm and

10 cm. A schematic diagram of the set up used is shown in figure 9.1.

9.3 Results and Discussions

Fig 9.2 shows a spectrum of 137Cs gamma rays taken using a NaI detector with

and without extra lead backing. Similarly, fig 9.3 shows the spectra taken using HPGe

detector, with and without extra copper backing behind the source. From the areas under

the photo peak and the back scattered peak of each gamma ray spectrum, the relative

yield of the back scattered peak has been obtained as a ratio of the areas of the relevant

peaks. Figures 9.4 and 9.5 give the variation of the relative yields of the back scattered

peaks as a function of the μt values of the backing for the two source to detector

distances for ^{137}Cs and ^{60}Co sources. Fig 9.6 give a similar plot for the ^{57}Co source, taken

with the HPGe detector.

The general trend of the plots in figures 9.4 – 9.6 is similar. As the backing

thickness increases, the relative back scattered yield increases and finally reaches a

saturation around μt = 0.5. This is the expected trend also. Moreover, it is seen that as

relative yield increases as the source to detector distance is decreased.

Backing   Source

Detector

Fig. 9.1 Schematic diagram of the experimental setup for study of the effect of source backing on the back scattered peak in gamma ray spectrum
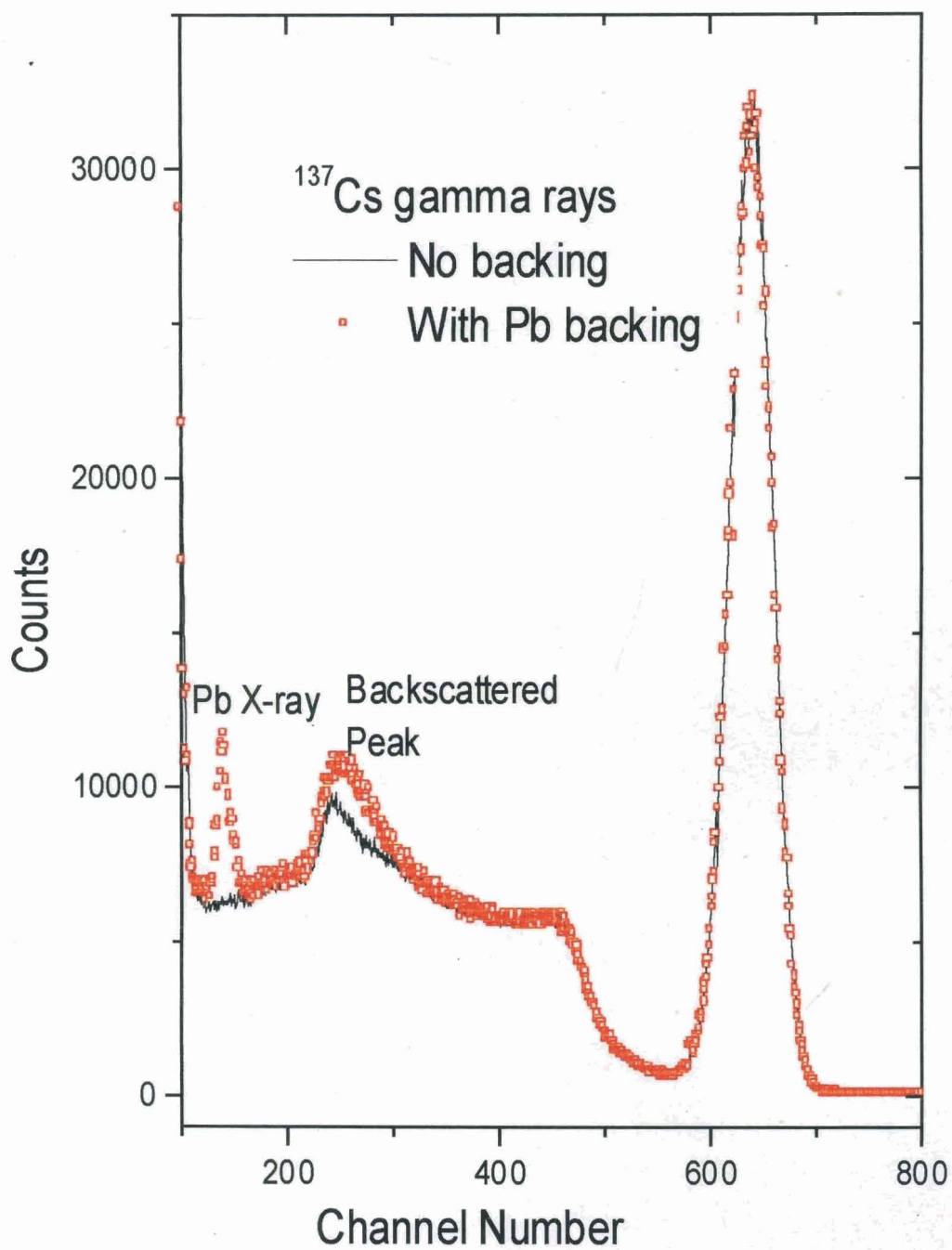
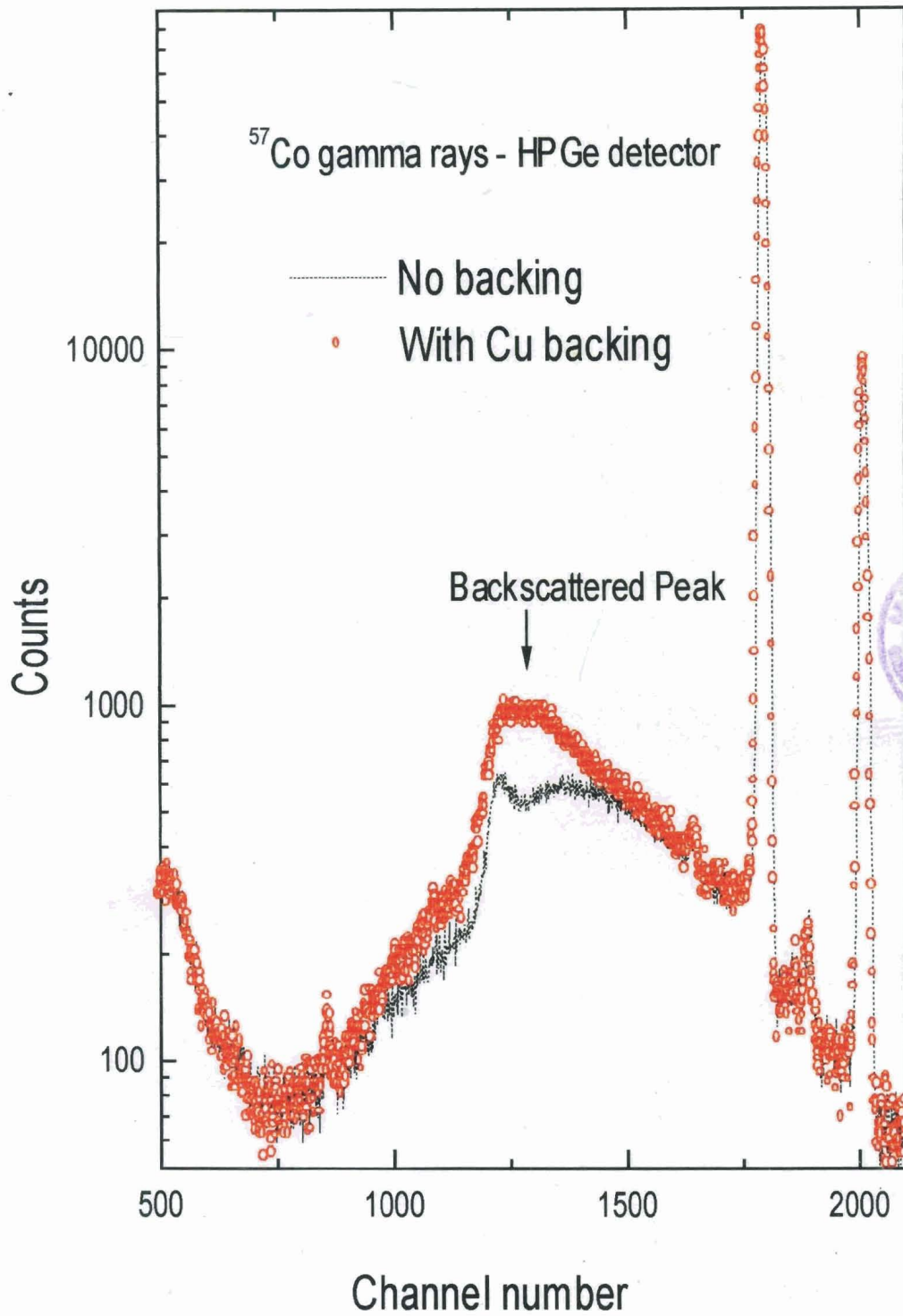Fig 9.2 - Spectrum of ^{137}Cs gamma rays with and without lead backing
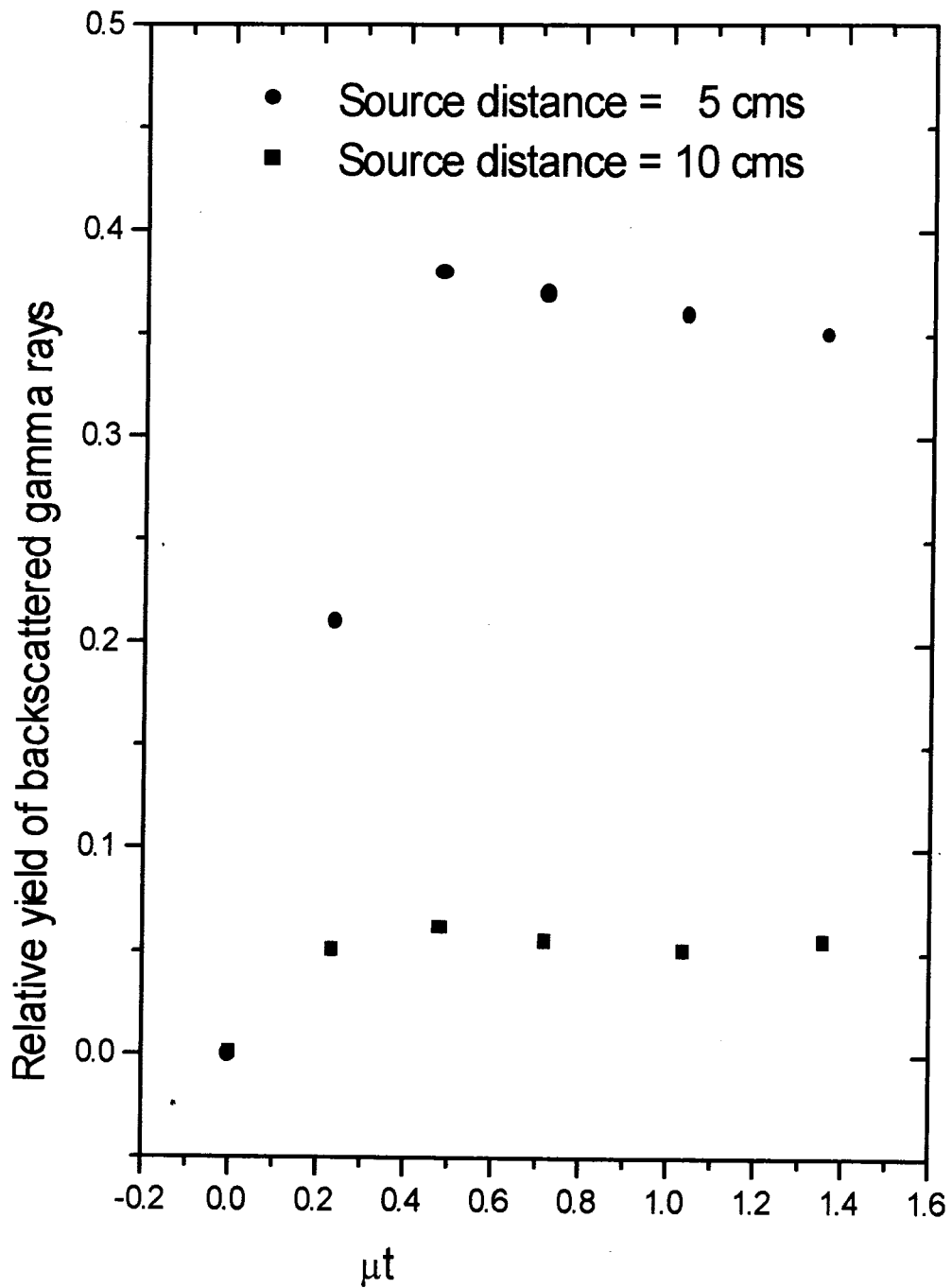
Fig 9.3 Spectrum of 57Co gamma rays with and without copper backing

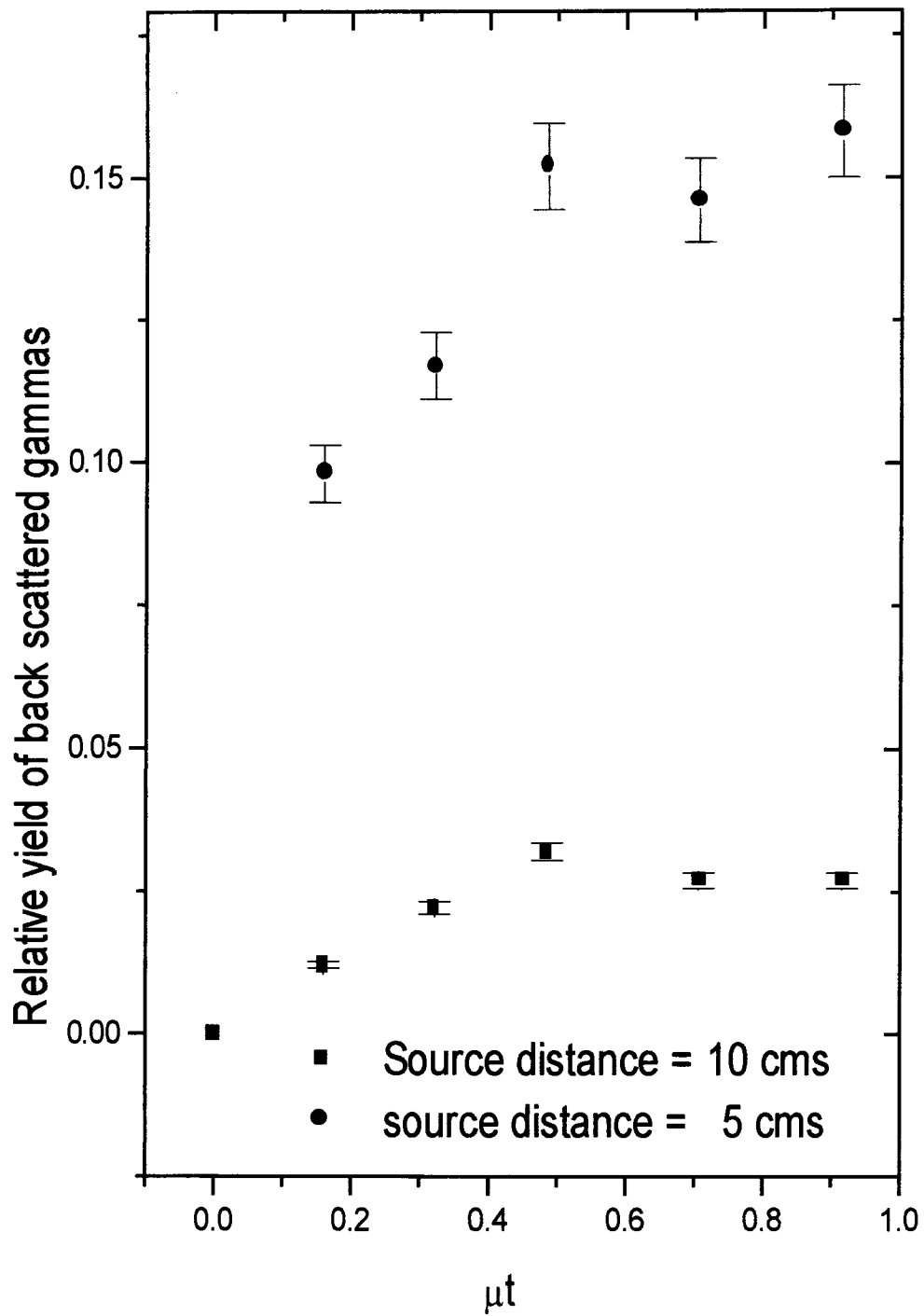Fig 9.4 - Relative yield of backscattered ^{137}Cs gamma rays (Pb backing)

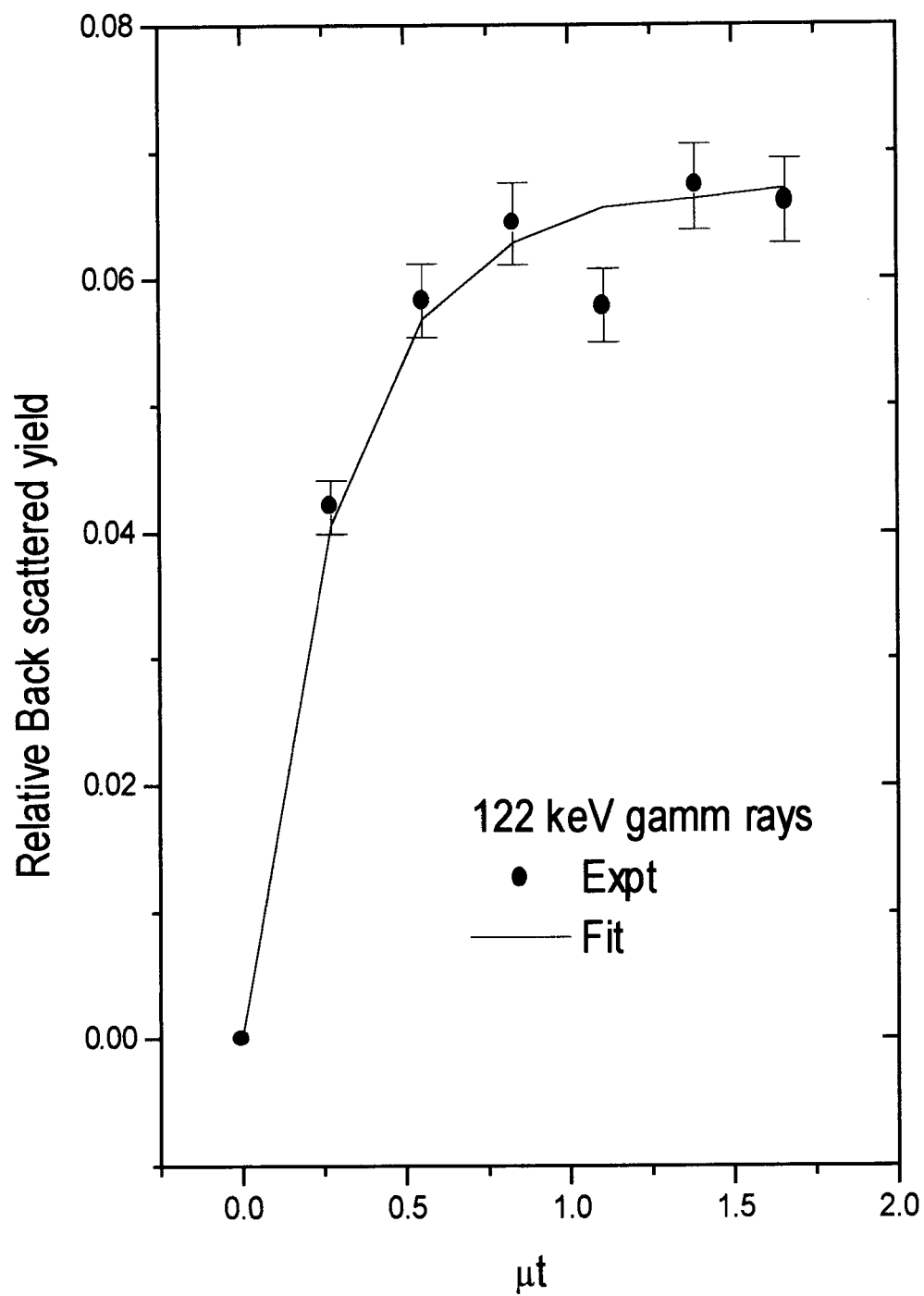Fig 9.5 - Relative yield of backscattered ^{60}Co gamma rays (Pb backing)

Fig 9.6 - Relative yield of back scattered gamma rays
as a function of μt values

REFERENCES

1. Knoll G.E., "Radiation Detection and Measurement", John Wiley & Sons (1989) p. 322, 784

2. Siegbahn K., "Alpha Beta and Gamma Ray Spectroscopy", North Holland Publishing Co., (1979) 256

NB 3248